Study on Flow Dynamics of Carbon Dioxide/Natural Gas in a Nanoporous Adsorbent-based Adsorption Column

by

Mohd Farhan Bin Alias
15503

Dissertation submitted in partial fulfilment of the requirement for the
Bachelor of Engineering (Hons)
(Chemical Engineering)

SEPTEMBER 2014

UniversitiTeknologi PETRONAS
Bandar Seri Iskandar
31750 Tronoh
Perak DarulRidzuan

CERTIFICATION OF APPROVAL

Study on Flow Dynamics of Carbon Dioxide/Natural Gas in a Nanoporous Adsorbent-based Adsorption Column

by

Mohd Farhan Bin Alias

15503

A project dissertation submitted to the

Chemical Engineering Programme

UniversitiTeknologi PETRONAS

In partial fulfilment of the requirement for the

BACHELOR OF ENGINEERING (Hons)

(CHEMICAL)

Approved by

_____

(Mr. Mohd Zamri Abdullah)

UNIVERSITI TEKNOLOGI PETRONAS

TRONOH, PERAK

September 2014

CERTIFICATION OF ORIGINALITY

This is to certify that I am responsible for the work submitted in this project, that the original work is my on except as specified in the references and acknowledgement, and that the original work contained herein have not been undertaken or done by unspecified sources or persons

_____

(MOHD FARHAN BIN ALIAS)

ABSTRACT

This study will investigate the flow dynamics of the carbon dioxide-natural gas flow in a nanoporous adsorbent-based adsorption column through computational approach. The process is simulated through the use of computational fluid dynamics (CFD) software by varying the process parameters such as particle diameter sizes, column geometry and column dimension. The proposed dimensional characteristic of the column to be studied is in a demo sized version, which is predicted to be about 50 times larger than the current studied lab-scale version. In this study, the actual adsorption rate of CO_2 by the nanoporous adsorbent is not considered, whereby the simulation is merely based upon the 'non-reactive' flow of the gases through a porous domain. It is expected that the analysis of the flow dynamics for the process would provide a viable information on the possible operating conditions for the demo scale adsorption column that would be used in the design of the actual version for the purification of CO_2 from natural gas.

ACKNOWLEDGEMENT

I would like to express my deepest gratitude to the Chemical Engineering department of UniversitiTeknologi PETRONAS (UTP) for providing the chance to undertake this remarkable Final Year Project (FYP). My knowledge and skills has been put to a test after completing various kinds of project during my five years intensive chemical engineering course. This course has a good coverage on the overall chemical engineering programme whereby a student with any majors has been assigned with different scope of the study thus contribute the effort and knowledge towards achieving a project goal.

Most important, a very special note thanks to my supervisor Mr. Mohd Zamri Abdullah, who was always willing to assist and provided good support throughout the project completion. Your excellent support, patience and effective guidance have helped my project to completion. I would like to thank to FYP1 and FYP2 coordinators, Dr Maziyar Sabet and Dr Asna respectively for arranging various seminars as support and knowledge to assist the group in the project. The seminars were indeed very helpful and insightful to us.

Besides that, I would also like to take this opportunity to express my deepest thanks to all laboratory technicians who had given guidance in completing this project experiment. Last but not least my heartfelt gratitude goes to my family and friends for providing me continuous support throughout the duration of this project.

Table of Contents

LIST OF FIGURES

LIST OF TABLES

CHAPTER 1: INTRODUCTION

1.1 Project Background

Natural gas (NG) is produced in the earth's crust by emitting the gas which is composed of 70-90% methane and also carbon dioxide (CO_2) witha composition of around 0-20%. It can be said that the majority of the NG composition is composed of methane and followed by carbon dioxide. Generally, high value of CO_2 in NG brings up several negative effects including reduction in NG heating value and also contribute to pipeline corrosion phenomena [1]. Thus, there are several scientific researches that have been developed throughout the world to find the most efficient way to remove CO_2 from NG such as gas absorption, cryogenic separation, membrane separation and adsorption system with the presence of alkanolamines as the physical solvent to absorb CO_2 [4].

It is alleged that adsorption is the most appropriate method to capture the CO_2 from NG [2]. There are many adsorbents that have been suggested for CO_2 adsorption including zeolites, activated carbons, silicas, hydrotalcites and metal oxides. These adsorbents are studied and investigated for their rate of CO_2 adsorption capacity, especially for activated carbons and zeolites. Both activated carbons and zeolites have been widely investigated due to their competitive CO_2 adsorption capacities [3].

Currently, there is limited research to investigate the full potential of the utilization of adsorbents from agricultural-based resources. Thus, considering Malaysia is a country that is rich in nature reserves, the agricultural wastes such as coconut shells, rice husk and bamboo stem has gained much attention over the last decade for the production of adsorbent based activated carbons by thermo-chemical conversion [7].

1.2 Problem Statement

The research to separate CO_2 from NG has been done for years and there are many studies that prove to be successful in removing the CO_2 from NG mixtures such as cryogenic distillation, membrane purification, absorption with liquids and adsorption using solids. However these methods are very different in their procedures compared to each other and their effectiveness to separate CO_2 from natural gas. This study will emphasizes on flow dynamics of CO_2 on its removal from NG in relation to different parameters such as particle diameter sizes, column geometry and column dimension. The simulation will be done on demo-scale and previous simulation on lab-scale and pilot-scale also will be reviewed as a basis in this study.

1.3 Objectives

To study the flow dynamics of the CO_2/NG in a demo-scale adsorption column and investigate the flow properties subjected to the variation of process parameters.

1.4 Scopes of study

- This study aims to apply systematic computational approach consisting of modeling work that expands into a process optimization and simulation of the adsorption column for CO_2 capture by nanoporous activated carbon developed from Malaysia agricultural wastes.

- The scopes of study also including the parameters of flow dynamics of CO_2 capture such as properties of fluid, velocity and pressure as functions of space and time.

CHAPTER 2: LITERATURE REVIEW

2.1 Carbon Dioxide Capture from Natural Gas

The existence of CO_2 in the NG has created disadvantages which decreases the efficiency and optimization of NG as a whole. Since then, researches have attempted various methods in order to maximize the purity of NG by applying several possible separation methods. Generally there are four main approaches to remove carbon dioxide from natural gas which include cryogenic distillation, membrane purification, absorption with liquids, and adsorption using solid adsorbents.

Cryogenic distillation, although widely used for other gas separations, is generally not considered as a practical means to separate carbon dioxide due to the high energy costs involved. Membranes have been extensively studied for carbon dioxide separation from relatively concentrated sources, such as natural gas deposits. Membranes can be highly efficient mass-separating agents, especially when the species that are to pass through the membrane are present in a large concentration. However, as carbon dioxide is a minor component of the off-gases, this method is unlikely to become the most efficient approach for the separation [8]. Instead, adsorption is proven as the best viable method for CO_2 removal from NG as it requires less energy, and provides high efficiency of CO_2 removal, ease of separation and simple in design [3].

2.2 Adsorbent from Agricultures

Activated carbon is a common term used for the absorption of substances in crystalline form which its properties includes the large internal pore structures that make the carbon more absorbent. In general, the raw materials for the production of activated carbon is originated from high carbon materials with low inorganic element such as wood, lignite, peat and coal. In addition, there are a lot of agricultural waste and by-products that have been successfully converted into activated carbon, such as macadamia nutshell paper mill sludge and peach stones. In Malaysia, the other possible alternative resources for

the production of activated carbon from agricultural wastes includes sugarcane bagasse, rice husk, palm kernel shells, coconut shell and palm fruit bunch [9].

Biomass has become the source of interest to create adsorbents that are environmental friendly. This is quite fascinating for this project as Malaysia has opened of more than 3 million hectares of oil palm plantations and that approximately 90 million metric ton of renewable biomass in the form of trunks, fronds and shells [5].

Several studies have been carried out to determine the best type of adsorbent for the removal of carbon dioxide from the mixture of CO_2 in NG is the Pressure Swing Adsorption (PSA) [3]. The adsorbent that is used is 13X zeolite which has been recognised as the most suitable adsorbent due to the higher adsorption capacity of CO_2 [6].

It also has been found that low cost carbons from biomass residue, olive stones and almond shells were created as adsorbents for carbon dioxide capture. These adsorbents were produced from biomass chars by two different methods: physical activation with carbon dioxide and amination. These adsorbents possess a high adsorption capacity at 303K although carbons developed from almond shells has a superior carbon dioxide over nitrogen selectivity than those obtained in olive stones [3].

Besides, good quality and sustainable activated carbons and carbon molecular sieves can be obtained from biomass precursors. The production of carbon adsorbents from biomass precursors involves either physical or chemical activation. In industry, it is quite familiar that this activated carbon is produced from wood by the phosphoric acid process; activation with potassium hydroxide is also frequent [7].

2.3 Simulation through Computational Fluid Dynamic (CFD) Approach

The dynamics behaviour of the CO_2 capture can be modelled and characterized using integrated CFD model [1]. The modelling approach describes an extrapolations of experimental results for conditions which is difficult and expensive to explore experimentally. In addition, kinetics modelling indicates the CO_2 uptake behaviour as a function of time, which gives comparison on uptake rate performance between different materials [6]. The modelling or simulation developed by CFD is best used when the process performance is determined by the fluid dynamics. CFD has been introduced as an advanced tool to model and simulate hydrodynamics, mass and heat transfer phenomena and design optimization of process equipment [1].

In order to reflect the CO_2 properties and behaviour towards the nanoporous particles, along with avoidance of high cost of experimental set-up for industrial scale-up, the intention is to develop the modelling of kinetic and equilibrium adsorption phenomena of adsorption column [1]. Navier-Stokes equations have been solved using CFD to observe the velocity profile and pressure gradient along the adsorption column [10].

Nouh*et al*. in his research usesan integrated CFD model to simulate transport phenomena of CO_2-NG fixed bed adsorption column and validated flow dynamics and mass transfer models with experimental data. The authors concluded that the dynamics within the packed beds significantly influences the performance and capability of the adsorption process [1]. They also studied on the kinetics of the adsorption experimentally, and found a good agreement to the model derived through CFD simulation [10].

The distinctive application for the CFD approach by Augier *et al*. has developed a CFD simulation tool to enable the study of coupling between flow dynamics and adsorption at different scales, ranging from laboratory to industrial scales. In the mathematical modelling, the mass transfer rate was modelled using a linear driving force (LDF) and for the flow dynamics, laminar Navier-Stokes equations were used by taking into account the friction between liquid and bed particles. The CFD model was validated

with experimental measurements [11].

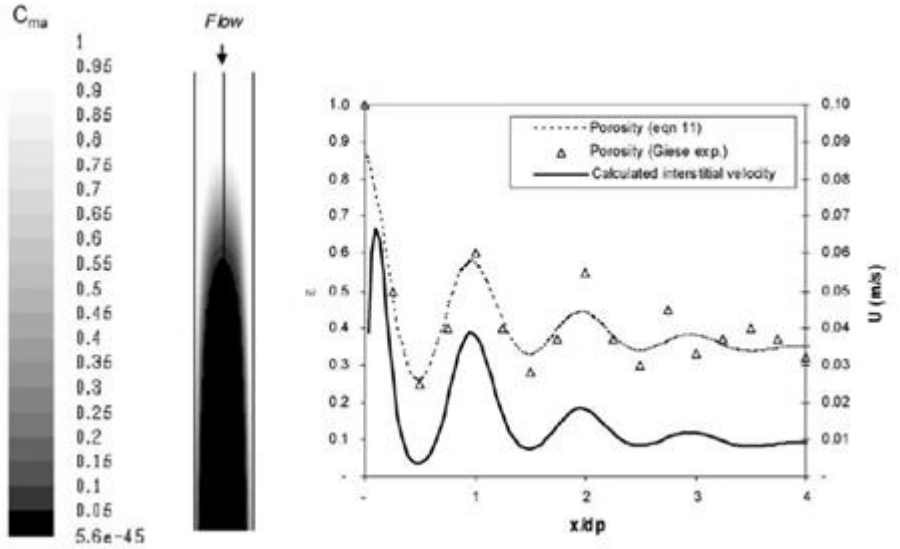

FIGURE 2.1: Simulation of a tracer flow (in white) inside a Φ 1 cm column. Left: Snapshot of the tracer concentration i.e. velocity, experimental and calculated. Right: Porosity profiles inside the column [11].

The application of CFD in the area of porous media for the adsorption of water on silica gel type B granules has been studied by White to explore the effect of granular size on the water adsorption rate and forecasting the water vapour flow pattern, temperature, heat transfer, flow velocity and adsorption rate through the use of SolidWorks® software. This is to study the characteristic of adsorbent which also become the main factor during the adsorption process. The CFD study and the experimental results were discovered to be in good agreement, which it was concluded that adsorptivity increases by reducing the granule size [10].

The findings of all of these researches on CFD can be summarize as below:

TABLE 2.1: The comparison of findings between the researchers

Author/year	Aspect	Brief Finding
S.A. Nouh, K.K Lau and	Comparison of Integrated CFD Approach and experimental set-up	This study showed that flow dynamics such as feed velocity, bed

A.M. Shariff / 2010	through Fixed Bed Adsorption Column.	porosity and inlet concentration within the fixed bed significantly influences the performance and capability of adsorption process.
M. Zamri Abdullah and S. Ali QasimZohair / 2014	Utilization of nanoporous adsorbent from agricultural waste for carbon dioxide capture through CFD.	The flow dynamics of CO_2 is investigated through adsorption column and the effect is observed with different scales which are pilot scale (smaller model) and demo scale (bigger model). Based on this study, the upscaling of scale from pilot to demo will increase the rate of velocity and pressure distribution inside adsorption column.
M. Hamudupour, J. Chen, and FaicalLarachi / 2012	Study on flow dynamics in three-phase fluidized beds through CFD.	CFD simulation of gas-liquid-solid fluidized beds were carried out by using a triple-Euler framework and the objective of the study to identify the effect of turbulence models is achieved.

CHAPTER 3: METHODOLOGY

The study on the flow dynamics of CO_2 in natural gas can be determined through the use of ANSYS CFX software and there is a sequence of steps that need to be done in order to ensure the objectives of the project is achieved. The process flow of the ANSYS CFX software can be described as below diagram:

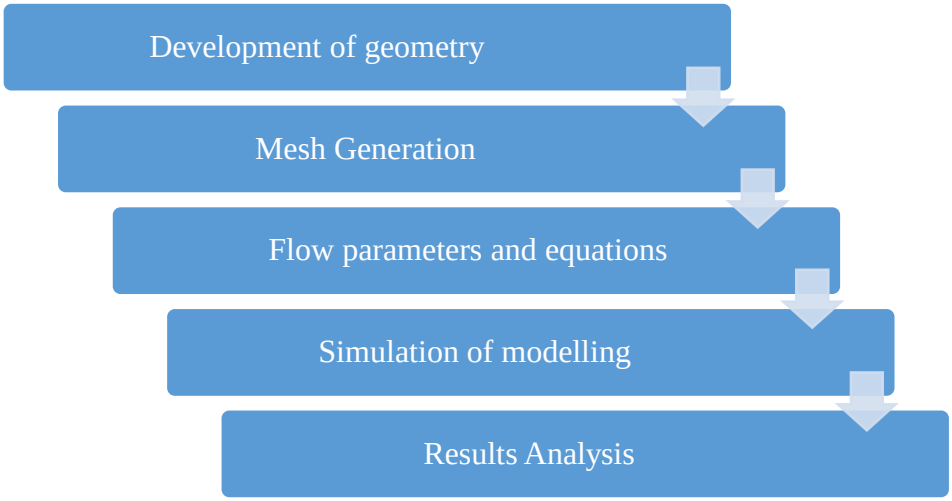

FIGURE 3.1: Process flow of ANSYS CFX simulation

The methodology include the creation of 3D flow domain of the demo-scale adsorption column; discretization of the numerical domain through the generation of mesh elements; setting up boundary conditions and solving the set of model equations through the ANSYS CFX software. The overall structure of the CFD simulation is simplified in the following flowchart.

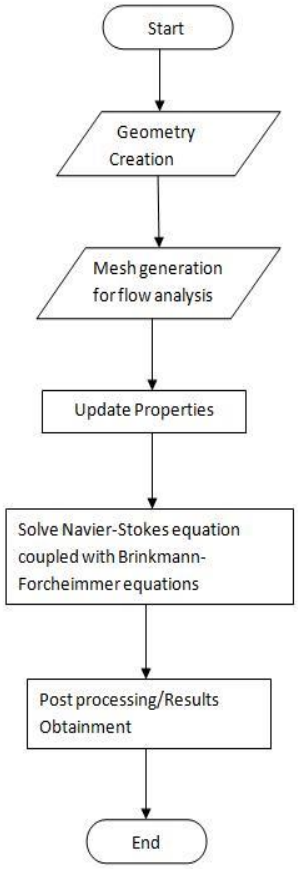

FIGURE 3.2: CFD simulation flowchart [10]

3.1 Tool & Software Required

Software

- ANYSS CFX

This is the commercial Computational Fluid Dynamics (CFD) program which is used to simulate fluid flow in a variety of application. The ANSYS CFX product enable engineers to test the systems into a virtual environment. The program has been applied to make simulation in various scale such as simulation of water flowing past ship hulls,

gas turbine engines (including the compressors, combustion chamber, turbines and afterburners), aircraft aerodynamics, pumps and other different simulations.

3.2 ANSYS CFX Simulation Process Description

The application of ANSYS CFX software covers the processes as shown in the Figure 3.2 above such as geometry creation, mesh generation for flow analysis, update properties, solving Navier-Stokes equation coupled with momentum equations and post processing.

3.3 Development of Geometry

Initiate the development of simulation through ANSYS CFX.

TABLE 3.1: Parameters of flow topology of Demo-scale modelling

Type	Demo-scale
Height	250 cm
Diameter	25 cm
Volume	122, 718 cm^3

3.3.1 Simulation through ANSYS CFX Software

The study of the flow dynamics of CO_2 in natural gas can be investigated through the simulation of the adsorption column in ANSYS CFX software. The adsorption columns were done in demo-scale and were developed for 3 geometries which the totaled volume for each geometry is 122, 718 cm^3. The main purpose is to examine the different in pressure drop and also velocity changes. The process will go through creation of geometry in Design Modeler, meshing of geometry and setup of design in CFX.

3.3.2 Geometry Creation through Design Modeller

The geometry 1 is created with dimension of 250 cm in height and 25 cm in diameter through Design Modeler in ANSYS CFX. It is full solid cylinder which simulate the solid cylinder of adsorption column. The creation of geometry 1 can be seen in Figure 3.3 below:

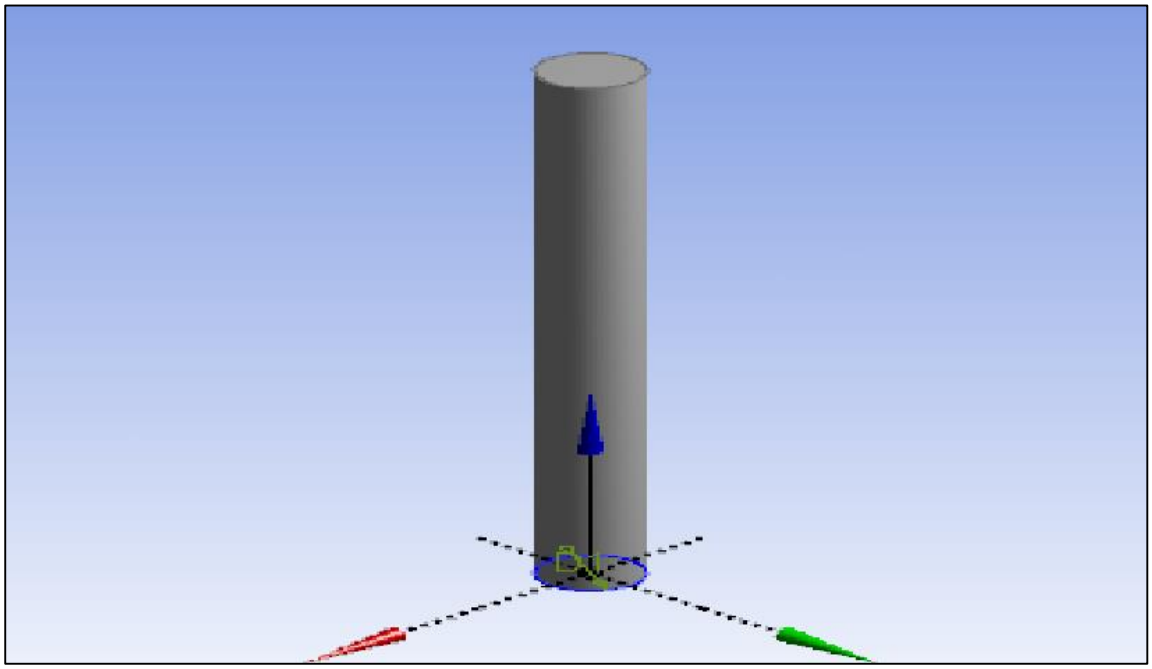

FIGURE 3.3: Solid Cylinder of Geometry 1

The geometry 2 is created with multi-cylinder solid with dimension of 250 cm in height and 9.45 cm of diameter. It is contains of 7 small multi-cylinder solids and simulated through Design Modeler in ANSYS CFX. The pattern of the small multi-cylinder is circular. The intention to develop multi-cylinder with circular shape is to observe the velocity and pressure behaviour around the circular shape throughout adsorption column compared to the common solid cylinder adsorption column. The creation of geometry 2 can be seen in Figure 3.4 below:

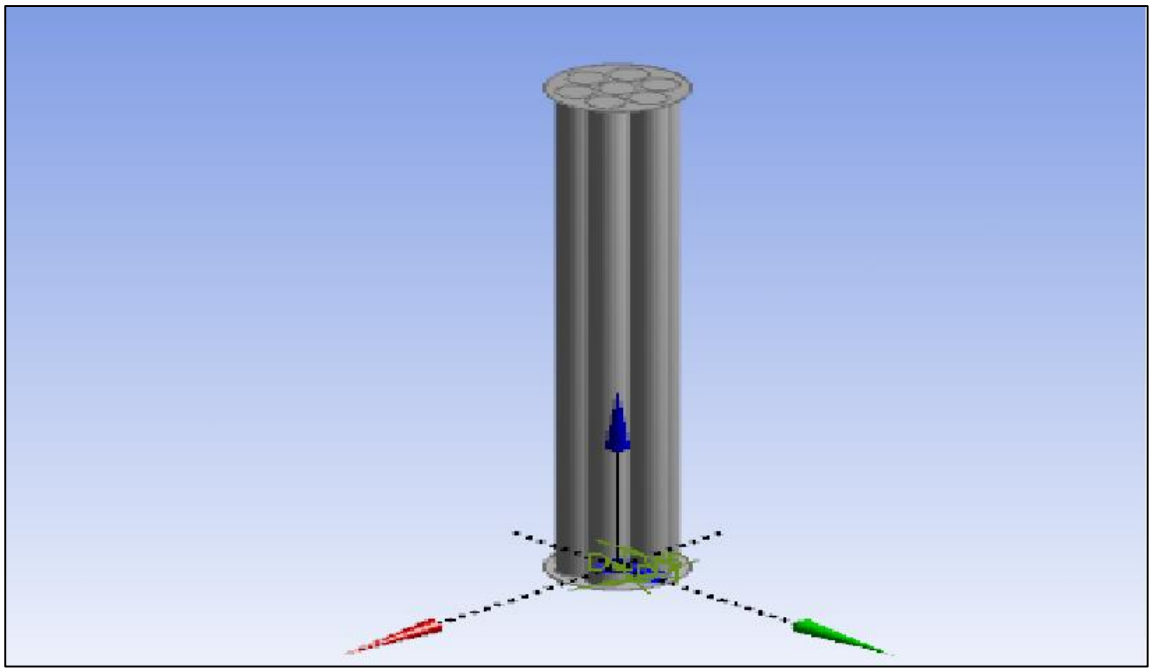

FIGURE 3.4: Multiple Solid Cylinder Circular Pattern Geometry 2

The geometry 3 is created with multi-cylinder solid with dimension of 250 cm in height and 8.33 cm of diameter. It is contains of 9 small multi-cylinder solids and simulated through Design Modeler in ANSYS CFX. The pattern of the small multi-cylinder is rectangular. The intention to develop multi-cylinder with rectangular shape is to observe the velocity and pressure behavior around the rectangular shape throughout adsorption column compared to the common solid cylinder adsorption column. The creation of geometry 3 can be seen in Figure 3.5 below:

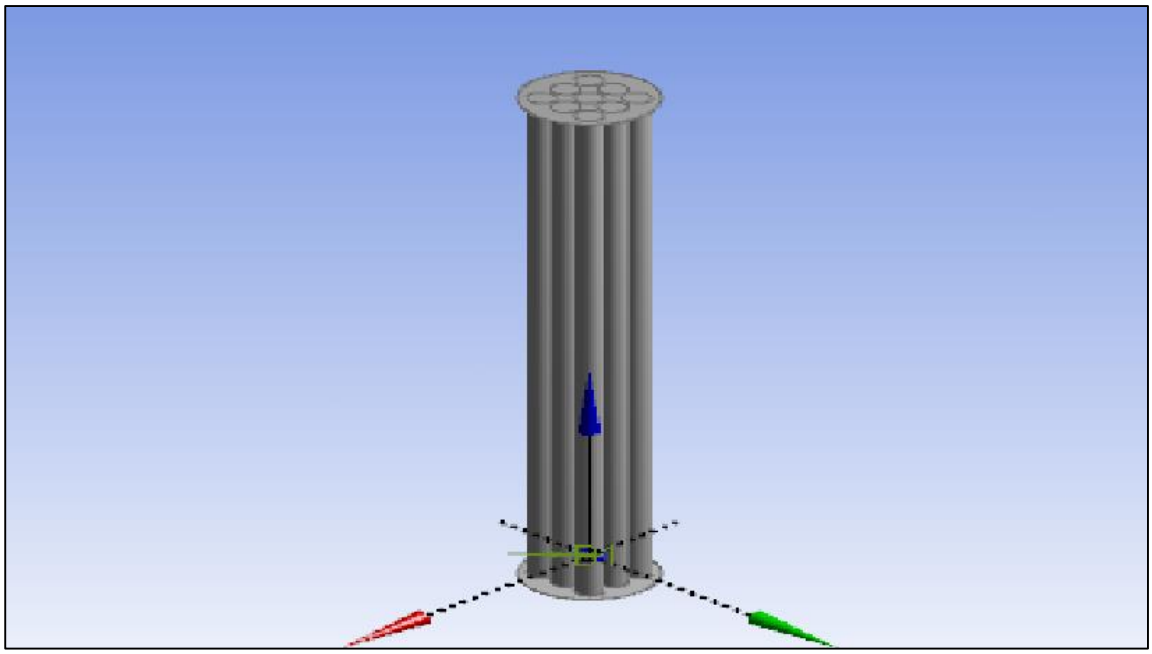

FIGURE 3.5: Multiple Solid Cylinder Rectangular Pattern Geometry 3

3.4 Mesh Generation for Flow Analysis

The 3D flow domain is discretized through the generation of mesh or grid. The mesh establishes the accuracy of simulation which should be chosen with enough detail to describe the simulation process accurately and enables to reach solution within an acceptable amount of time. Hence, the grid generation influences the computational time and the ability of CFD to predict the conditions [5]. In this study, the expected mesh generated is as figure below which shows the axial and radial mesh configuration.

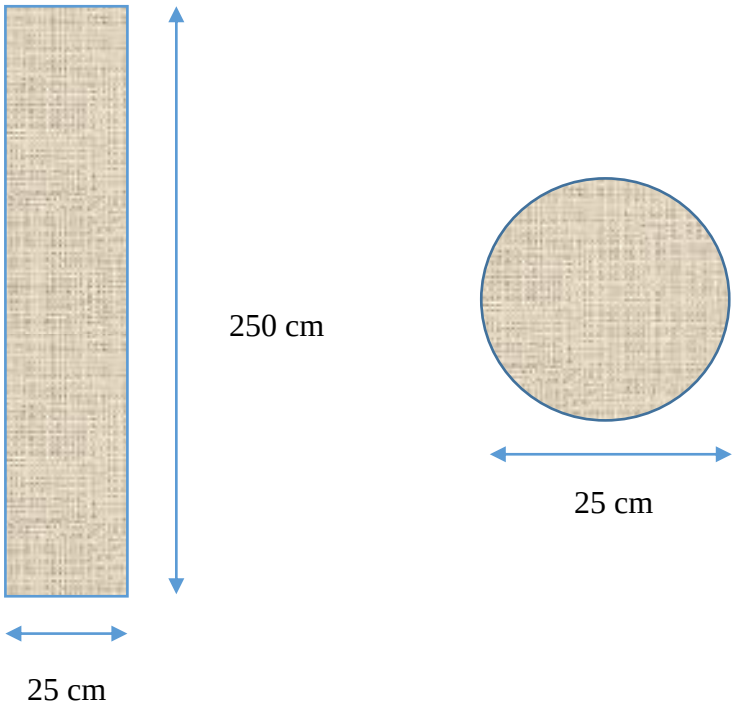

FIGURE 3.6: Axial and radial mesh configuration

Meshing is the process of uniformity and establishes the accuracy of simulation which be chosen with enough detail to describe the simulation process accurately and enables the solver to achieve the solution within an acceptable amount of time. In this study the mesh has been generated in ICEM CFD14.5 for uniformity. A domain with 200,440 nodes, 524,836 nodes and 538,636 nodes were generated for geometry 1, geometry 2 and geometry 3 respectively. The meshing grid optimization can be seen as figure below:

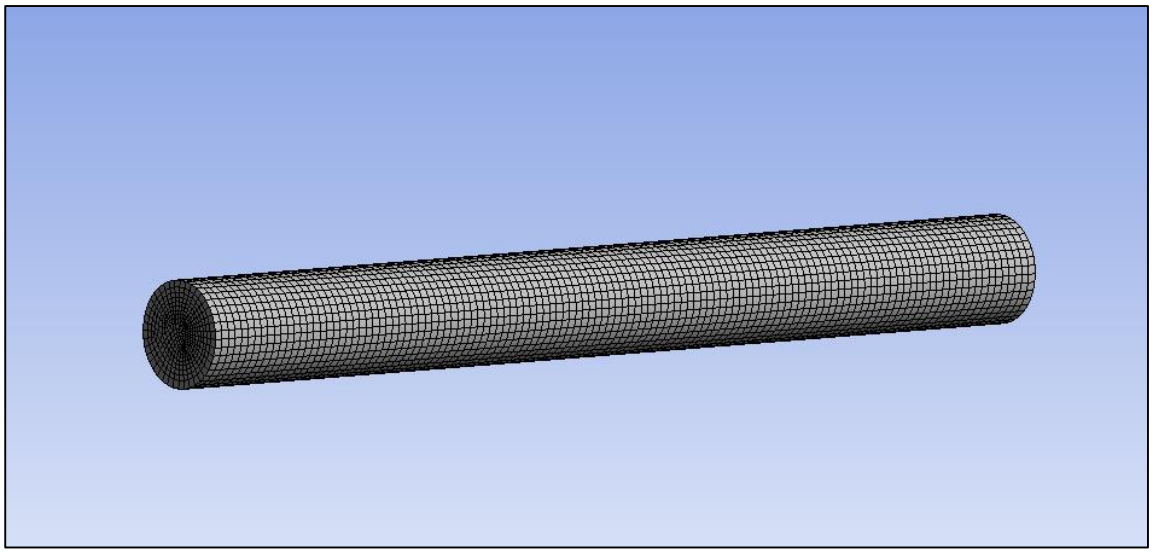

FIGURE 3.7: Generation of Mesh for Geometry 1

Details of "Mesh"	
Use Advanced Size Fun...	On: Curvature
Relevance Center	Fine
Initial Size Seed	Active Assembly
Smoothing	High
Transition	Fast
Span Angle Center	Fine
Curvature Normal A...	Default (18.0 °)
Min Size	5.e-003 m
Max Face Size	2.e-002 m
Max Size	2.e-002 m
Growth Rate	Default (1.850)
Minimum Edge Length	0.78540 m
Inflation	
Patch Conforming Options	
Patch Independent Options	
Advanced	
Defeaturing	
Statistics	
Nodes	200440
Elements	47875
Mesh Metric	None

FIGURE 3.8: Meshing Setting for Geometry 1

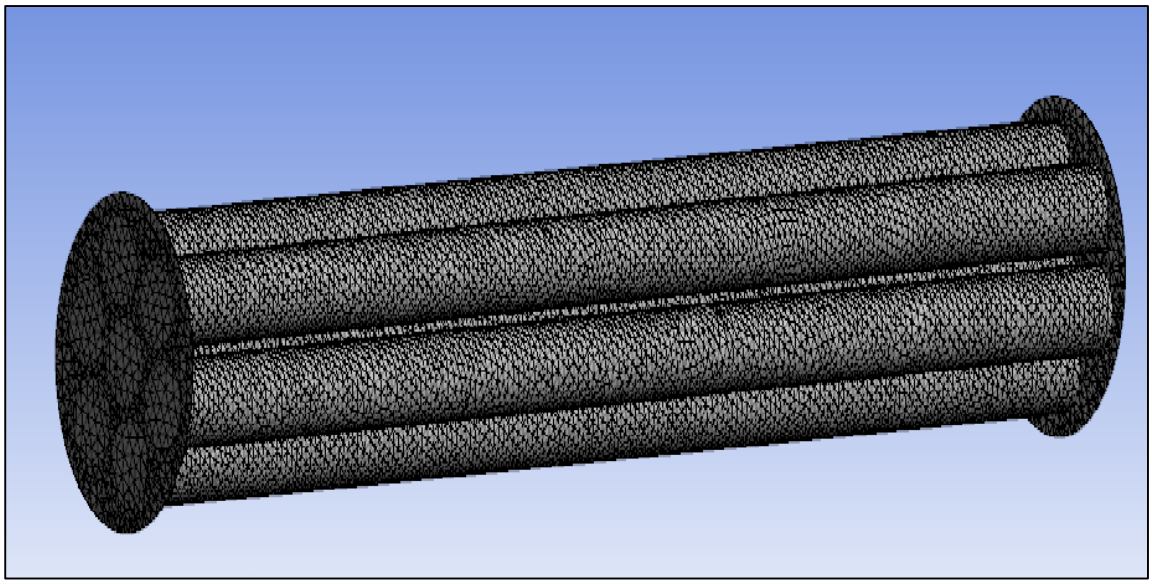

FIGURE 3.9: Generation of Mesh for Geometry 2

Details of "Mesh"	
Use Advanced Size Function	On: Curvature
Relevance Center	Fine
Initial Size Seed	Active Assembly
Smoothing	High
Transition	Fast
Span Angle Center	Fine
Curvature Normal Angle	Default (15.3750 °)
Min Size	6.e-003 m
Max Face Size	2.e-002 m
Max Size	2.e-002 m
Growth Rate	Default (1.73440)
Minimum Edge Length	0.296880 m
Inflation	
Patch Conforming Options	
Patch Independent Options	
Advanced	
Defeaturing	
Statistics	
Nodes	524836
Elements	335528
Mesh Metric	None

FIGURE 4.0: Meshing Setting for Geometry 2

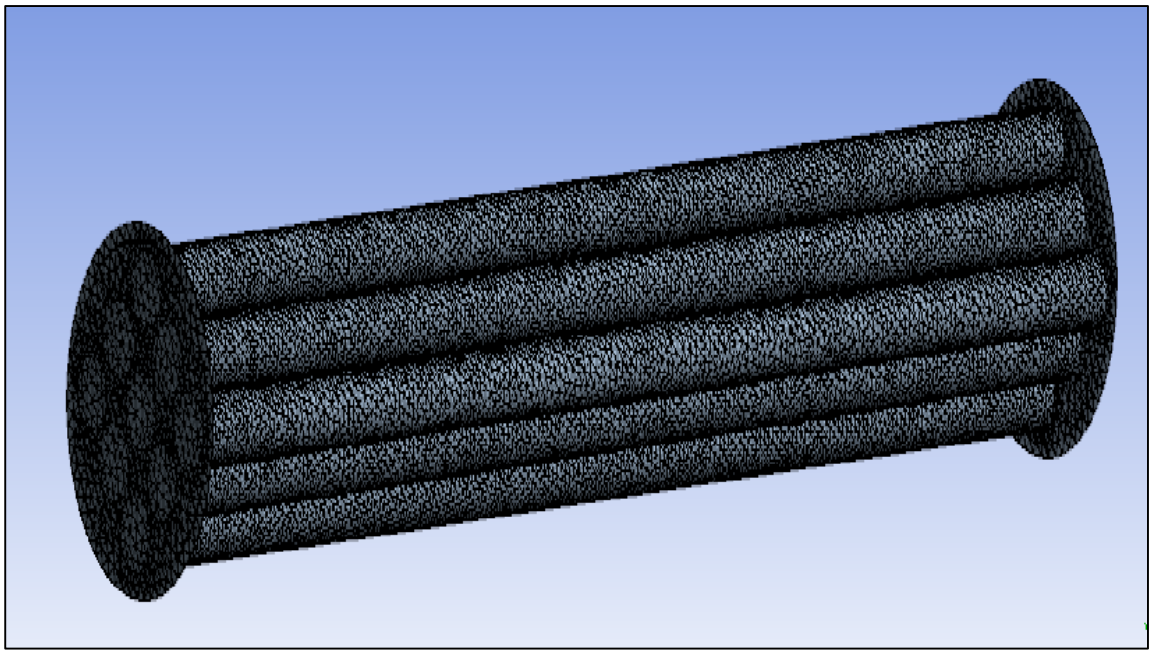

FIGURE 4.1: Generation of Mesh for Geometry 3

Details of "Mesh"	
Use Advanced Size Fun...	On: Curvature
Relevance Center	Fine
Initial Size Seed	Active Assembly
Smoothing	High
Transition	Fast
Span Angle Center	Fine
Curvature Normal A...	Default (18.0 °)
Min Size	7.e-003 m
Max Face Size	2.e-002 m
Max Size	2.e-002 m
Growth Rate	Default (1.850)
Minimum Edge Length	0.261690 m
Inflation	
Patch Conforming Options	
Patch Independent Options	
Advanced	
Defeaturing	
Statistics	
Nodes	538636
Elements	339834
Mesh Metric	None

FIGURE 4.2: Meshing Setting for Geometry 3

3.5 Setup and Update Properties in CFX

After finished with the geometry creation and generation of mesh, the properties were updated in the setup as shown in Table 3.2 below before generating the solver.

TABLE 3.2: Flow properties of Adsorption Column

Parameters	**Value**
Fluids	CO_2 (Ideal gas) CH_4 (Ideal gas)
Fluid Morphology	Continuous Fluids
Reference Pressure	1 atm
Heat Transfer Model	Isothermal
flow rate	2500 cm^3/min
Mass Diffusivity	2.88 x 10^{-5} m^2/s
Bed porosity, ε	0.34
Particle diameter, $D_{P,i}$	250 μm 500 μm

3.5.1 CFX Setting (Flow Analysis)

The CFX setting of flow analysis for 250 μm and 500 μm can be seen in the **APPENDIX A** and **APPENDIX B**.

3.6 Flow Parameter & Equation

Flow in porous media in ANSYS CFX can be calculated using either a model for momentum loss or a full porous model. The fluid domains is available for momentum loss model while the porous domains is available for porous loss model. The

simplication of the Navier-Stokes equations and of Darcy's law commonly used for flows in porous regions. It is been used when the geometry is too complicated to resolve with a grid. The model retains both advection and diffusion terms and can therefore be used for flows in rod or tubes bundles where such effects are significant [10].

In deriving the continuum equations, it is assumed that 'infinitesimal' control volumes and surfaces are large relative to the interstitial spacing of the porous medium, though small relative to the scales that you wish to resolve. Thus, given control cells and control surfaces are assumed to contain both solid and fluid regions. The volume porosity at a point is the ratio of the volume available to flow in an infinitesimal control cell surrounding the point, and the physical volume of the cell. The model used for the hydrodynamics combines laminar Navier-Stokes equations with momentum equation model to simulate flow in porous media [10].

Continuity equation: the general 3-D continuity equation for unsteady-state fluid flow is:

$$\frac{\partial \rho}{\partial t} + \frac{\partial \rho u}{\partial x} + \frac{\partial \rho v}{\partial y} + \frac{\partial \rho w}{\partial z} = 0 \qquad (1)$$

Navier-stokes equations

To represent the fluid flow through the porous medium, additional sources term S_{ix}, S_{iy}, S_{iz} were added to Eq. (2) - (4) to model the flow resistance in 3D dimensions as follow:

Navier-stokes equation in x-direction

$$\frac{\partial(\rho u)}{\partial t} + \frac{\partial(\rho u u)}{\partial x} + \frac{\partial(\rho v u)}{\partial y} + \frac{\partial(\rho w u)}{\partial z} = \frac{\partial P}{\partial t} + 2\frac{\partial}{\partial x}\left(u\frac{\partial u}{\partial x}\right) - \frac{2}{3}\frac{\partial}{\partial x}\left[u\left(\frac{\partial u}{\partial x} + \frac{\partial v}{\partial y} + \frac{\partial w}{\partial z}\right)\right] + \frac{\partial}{\partial y} + [u(\frac{\partial u}{\partial y} + \frac{\partial v}{\partial x})] + \frac{\partial}{\partial z}\left[u\left(\frac{\partial u}{\partial z} + \frac{\partial w}{\partial x}\right)\right] + S_{ix} \qquad (2)$$

Navier-stokes equation in y-direction

$$\frac{\partial(\rho v)}{\partial t}+\frac{\partial(\rho v v)}{\partial y}+\frac{\partial(\rho u v)}{\partial x}+\frac{\partial(\rho w v)}{\partial z}=\frac{\partial P}{\partial y}+2\frac{\partial}{\partial y}\left(u\frac{\partial v}{\partial y}\right)-\frac{2}{3}\frac{\partial}{\partial y}\left[u\left(\frac{\partial u}{\partial x}+\frac{\partial v}{\partial y}+\frac{\partial w}{\partial z}\right)\right]+\frac{\partial}{\partial x}\left[u\left(\frac{\partial v}{\partial x}+\frac{\partial u}{\partial y}\right)\right]+\frac{\partial}{\partial z}\left[u\left(\frac{\partial v}{\partial z}+\frac{\partial w}{\partial y}\right)\right]+S_{iy} \quad (3)$$

Navier-stokes equation in z-direction

$$\frac{\partial(\rho w)}{\partial t}+\frac{\partial(\rho w w)}{\partial z}+\frac{\partial(\rho u v)}{\partial x}+\frac{\partial(\rho v w)}{\partial y}=\frac{\partial P}{\partial z}+2\frac{\partial}{\partial z}\left(u\frac{\partial w}{\partial z}\right)-\frac{2}{3}\frac{\partial}{\partial z}\left[u\left(\frac{\partial u}{\partial x}+\frac{\partial v}{\partial y}+\frac{\partial w}{\partial z}\right)\right]+\frac{\partial}{\partial x}\left[u\left(\frac{\partial w}{\partial x}+\frac{\partial u}{\partial z}\right)\right]+\frac{\partial}{\partial y}\left[u\left(\frac{\partial w}{\partial y}+\frac{\partial v}{\partial z}\right)\right]+S_{iz} \quad (4)$$

The porous medium momentum source term S_i calculates the pressure gradient in the packed bed and creates a pressure drop that is proportional to the fluid velocity (or velocity squared) as shown below:

$$S_i=\frac{u}{\alpha}u_i+C_2\left(\frac{1}{2}\rho u_i|u_i|\right) \quad (5)$$

$$C_2=\frac{1.75}{D_p}\frac{(1-\varepsilon)}{\varepsilon^3} \quad (6)$$

$$\alpha=\frac{D_p^2}{150}\frac{\varepsilon^3}{(1-\varepsilon)^2} \quad (7)$$

Where, C_2 and α, are the inertia resistance and viscous resistant coefficient, which estimated using Eq. (6) and Eq. (7).

For continuity:

$$\tilde{\nabla}U=0 \quad (8)$$

For momentum

$$\frac{\partial \varepsilon U}{\partial t} + \nabla(\varepsilon \rho UU) = -\boldsymbol{\varepsilon} \mathrm{u} \nabla^2 \mathrm{U} + \varepsilon \mathrm{F} \quad (9)$$

Where 'F' represents fluid-particle friction forces:

$$F = \frac{uU_{sl}}{K} - \beta \rho U_{sl}^2 \quad (10)$$

For fluid particle friction forces, K is the permeability of porous media and β is the non-Darcy term or inertial resistance coefficient. In a fixed bed of narrow sized spheres, it is recommended to calculate K and β from the Ergun Eq. [11]:

According to Ergun's law, permeability K is expressed as:

$$K = \frac{\varepsilon^3 D^2{}_p}{150(1-\varepsilon)^2} \quad (11)$$

The expression of inertial resistance coefficient 'β' can be stated as:

$$\beta = 1.75 \frac{1-\varepsilon}{\varepsilon^3 D_p} \quad (12)$$

The value of permeability K for 250μm particles diameter which is inserted into the CFX setup is as below:

$$K = \frac{\varepsilon^3 D^2{}_p}{150(1-\varepsilon)^2}$$

$$K = \frac{(0.34)^3 (0.00025)^2}{150(1-0.34)^2} = 3.76\, x\, 10^{-11} m^2$$

Meanwhile, the value of inertial resistance coefficient ‘β’ for 250μm particles diameter which is inserted into the CFX setup is as below:

$$\beta = 1.75\left[\frac{1-\varepsilon}{\varepsilon^3 D_p}\right]$$

$$\beta = 1.75\left[\frac{1-0.34}{(0.34)^3(0.00025)}\right] = 117{,}545.29\ m^{-1}$$

The value of permeability K for 500μm particles diameter is calculated as:

$$K = \frac{(0.34)^3(0.0005)^2}{150(1-0.34)^2} = 1.50\ x\ 10^{-10} m^2$$

The calculation for inertial resistance coefficient ‘β’ for 500μm particles diameter based on below:

$$\beta = 1.75\left[\frac{1-0.34}{(0.34)^3(0.0005)}\right] = 58{,}772.64 m^{-1}$$

The porous media model incorporates an empirically determined flow resistance in a region of the model defined as ‘porous’. In essence, the porous media model is nothing more than an added momentum sink in the governing momentum equations. Porous media simulation is performed at Demo-scale. Three different adsorbent sizes have been selected that include particle sizes of 250 μm, 500 μm. The inlet flow rate is 2500 cm^3/min. The flow rate is taken form the basis of previous lab-scale as the demo-scale is 50 times larger than the lab-scale [10]. It is suggested that for cylindrical vessels with $D_t/D_p > 2$ and FGB height $H > 20d$, the bed porosity can be approximated by the expression:

$$\varepsilon = \frac{A}{(\frac{D_t}{D_p})^n} + B \qquad (13)$$

Where A, B and n are constants dependent on the shape of particle. D_t and D_p are the column and particle diameter respectively. Assuming the adsorbent particles are uniform and in a shape of sphere, the values of coefficients A, B and n are taken as 1.0, 0.375 and 2, respectively; resulting in the bed porosity, ε, is 0.34 [10].

In this section, the velocity and pressure profiles for the demo-scale adsorption columns are considered. The pressure gradient inside porous domain depends upon the factors of permeability and resistance coefficient along with viscosity, density and inlet velocity of the fluid. Andrade and others modelled gas flow in disordered porous media based on the Reynolds number defined as:

$$Re = \frac{K\beta pv}{u} \tag{14}$$

where the constants K and β have been previously defined. For the above used approach, the emergence of critical Reynolds number is 0.01 – 0.1 [10].

3.6.1 Velocity Distribution in Adsorption Column

Velocity profile is used to measure the flow conditions of fluids within the pipe. It is dependent on the value of Reynolds number that is being used which in turn depends upon the inlet velocity, diameter of the column, viscosity and density of fluid. The inlet superficial velocity is obtained by dividing the total volumetric flow rate with cross-sectional area. In this case, interstitial velocity profile is first simulated and is used to measure the flow conditions of fluid within the demo-scale geometry. In the presence of porous medium, the interstitial velocity will always be higher than the superficial velocity and represents the original change in velocity taken place inside the column. In this study, the gaseous mixture enters the porous domain at a volumetric flow rate of 2500 cm^3/min. For all simulation purposes, the fluid domain has been solved while considering porous media conditions for interstitial velocity. It is the actual velocity of fluid particles inside the domain. The superficial velocity and interstitial velocity, also

called as true velocity are easily related via;

$$V_s = \varepsilon . V_t \tag{15}$$

where 'V_s' is superficial velocity, 'V_t' is true velocity and 'ε' denotes porosity which is usually an isotropic property [10].

3.6.2 Pressure Distribution in Adsorption Column

Pressure gradient signifies the acceleration of gas due to pressure difference and the rate at which pressure changes most rapidly around a particular location. Pressure drop is an important parameter of fluid flow to measure the required energy consumption through fixed bed. The resistance to fluid flow gives rise to a pressure drop in the fluid given as ΔP. Pressure is not a vector quantity but the pressure gradient with respect to the distance (ΔP/L) is a vector quantity. The pressure decreases in the direction of fluid velocity so the pressure gradient is negative but if taken in terms of pressure difference, which is a scalar quantity, negative sign is not used for practical purposes. In some of the previous works, pressure drop for fixed bed adsorbers is considered negligible but there is also argument that this approach is not surely valid for processes that combine high flow rates and small particle diameter.

The pressure gradient inside porous domain depends upon the factors of permeability and resistance coefficient along with viscosity, density and inlet velocity of the fluid. Permeability and inertial resistance coefficient depend upon two variables which are bed porosity and particle diameter. In this case, the values for permeability and resistance coefficients have been calculated according to Ergun's law [10].

Andrade and others modelled gas flow in disordered porous media where the Reynolds number is written in terms of permeability, inertial resistance coefficient, density, velocity and viscosity of fluid.

$$Re = \frac{K\beta pv}{u} \tag{16}$$

For the above used approach, the emergence of critical Reynolds number is 0.01-0.1 [13].

3.7 Key Milestones

Final Year Project 1															
No	**Item/Week**	**1**	**2**	**3**	**4**	**5**	**6**	**7**	**8**	**9**	**10**	**11**	**12**	**13**	**14**
1	Determination of concept of flow dynamics of CO_2														
2	Various research through journals and books														
3	Determination of parameters (flow dynamics of CO_2)														
4	Simulation of model through ANYSIS CFX														
5	Analysis of Results														

3.8 Gantt Chart

Final Year Project 1															
No	**Item/Week**	**1**	**2**	**3**	**4**	**5**	**6**	**7**	**8**	**9**	**10**	**11**	**12**	**13**	**14**
1	Project title selection														
2	Background study and literature reviews on the fluid flow of CO_2 in natural gas														
3	Identifying suitable methodology in respect of several parameters														
4	Extended proposal														
5	Study on the parameters needed (fluid flow: fluid properties, velocity and concentration)														
6	Proposal defence														

7	Familiarize with simulation software (ANYSIS CFX)														
8	Develop the simulation and analyse the results														
9	Draft report submission														
10	Final report submission														
Final Year Project 2															
No	**Item/Week**	**1**	**2**	**3**	**4**	**5**	**6**	**7**	**8**	**9**	**10**	**11**	**12**	**13**	**14**
11	Develop the adsorption column model through simulation of ANYSIS CFX														
12	Perform the modelling and analyse result														

CHAPTER 4: RESULTS AND DISCUSSION

The results obtained has been analyzed and discuss in this chapter as the flow dynamics behavior of the CO_2 in NG is being examined in this study. The results obtained is based on demo-scale adsorption column which is approximately 10 times larger than pilot-scale and 50 times larger than lab-scale. Previous study regarding pilot-scale and lab-scale is also being considered as a fundamental of this study. Based on preceding research, the up-scaling sizes and parameters from lab-scale to pilot scale proved that velocity is increases by 10 times and pressure drop in the system escalates more than 1000 times than the former.

4.1 Velocity Distribution in Adsorption Column

Velocity profile is being investigated to define and measure the flow condition of the fluids in the adsorption column. The most significant factor in determining the velocity profile is based on the Reynolds number that is being used which directly depends on the inlet velocity, diameter of the column, viscosity and density of the fluid. The equation used is based on Eq. (16) which has been stated earlier and it is composed of an expression from Ergun's equation. The permeability 'K' and inertial resistance coefficient 'β' comes from expression in Eq. (11) and Eq. (12).

In this study, as porous medium is being used for the domain of the geometry model, theoretically it can be said that the interstitial velocity will always be higher than the superficial velocity and be considered as the true change of velocity taken place inside the column. The demo-scale column dimension has been created for all the geometriessimulated in this study. The inlet for the all of geometry models have been inserted with velocity of $2.12\frac{m}{s}$.

4.1.1 Axial Velocity Contour of 250μm Particles Diameter

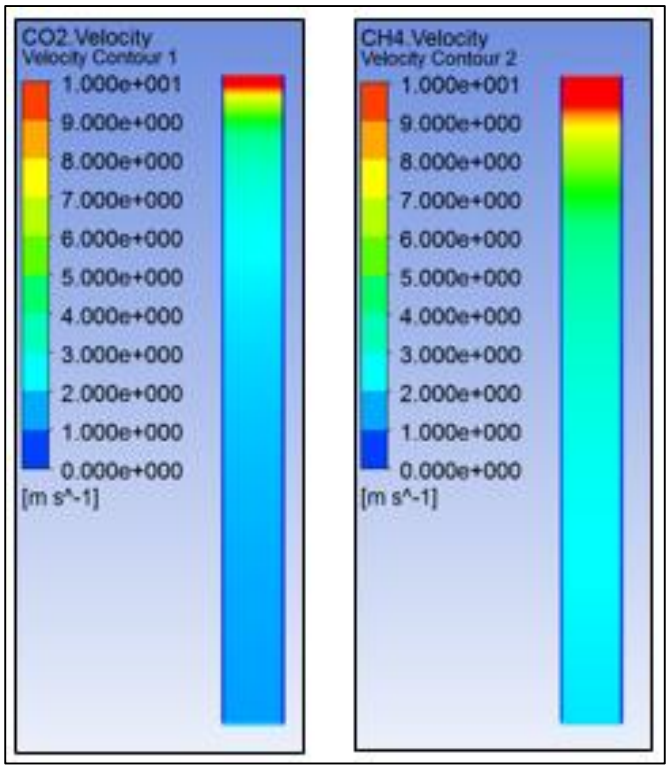

FIGURE 4.3: Geometry 1 Contour

The velocity contour is sliced at the centre of adsorption column at XY plane with coordinate of Z=0. The fluid velocity contour showing medium velocity flowrate from the inlet to the middle of column and exiting at high velocity towards the end of the column.

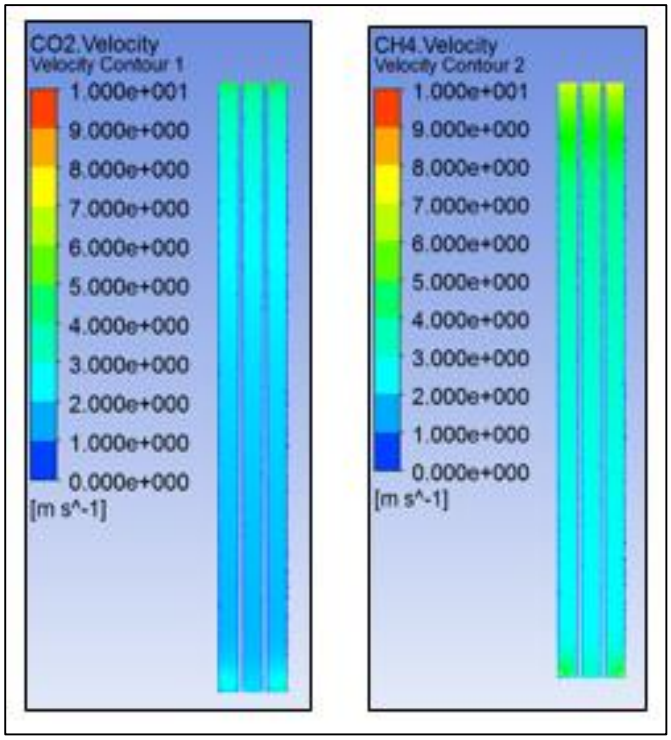

FIGURE 4.4: Geometry 2 Contour

The velocity contour is sliced at the centre of adsorption column at XY plane with coordinate of Z=0. The fluid velocity contour showing medium velocity flowrate throughout the column but the CH_4 velocity is showing higher velocity rate at the inlet and outlet of the column compared to CO_2 velocity rate.

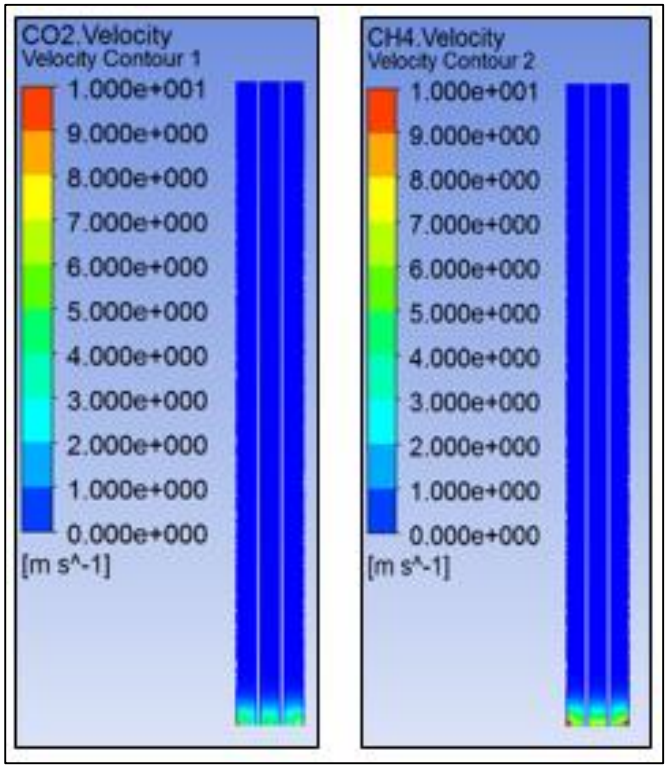

FIGURE 4.5: Geometry 3 Contour

The velocity contour is sliced at the centre of adsorption column at XY plane with coordinate of Z= 0.0933 m. Both fluid velocity contour showing medium velocity flowrate at the inlet of the column and reduces greatly to zero until the end of the column.

4.1.2 Axial Velocity Contour of 500µm Particles Diameter

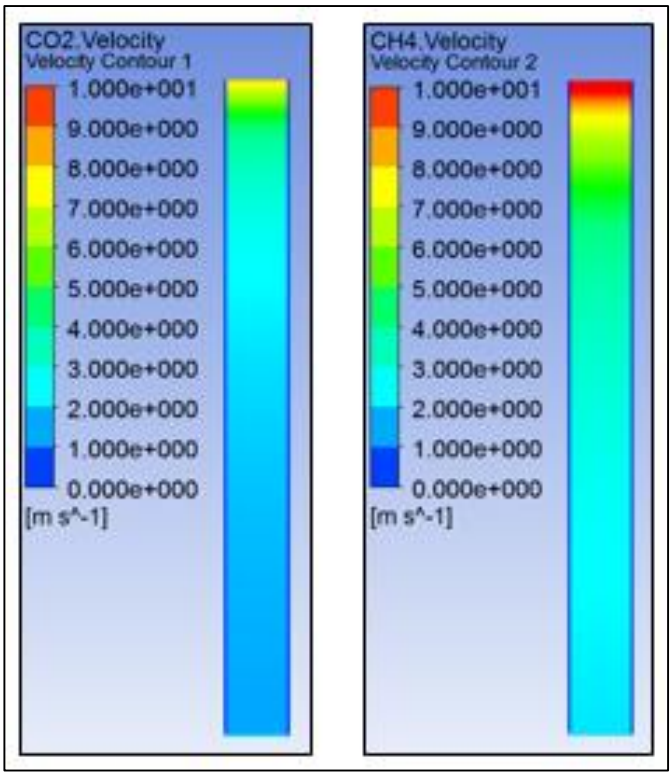

FIGURE 4.6: Geometry 1 Contour

The velocity contour is sliced at the centre of adsorption column at XY plane with coordinate of Z=0. Both velocity contour showing medium velocity speed from the inlet but CH_4 exiting at high velocity speed than the CO_2 at the end of the adsorption column.

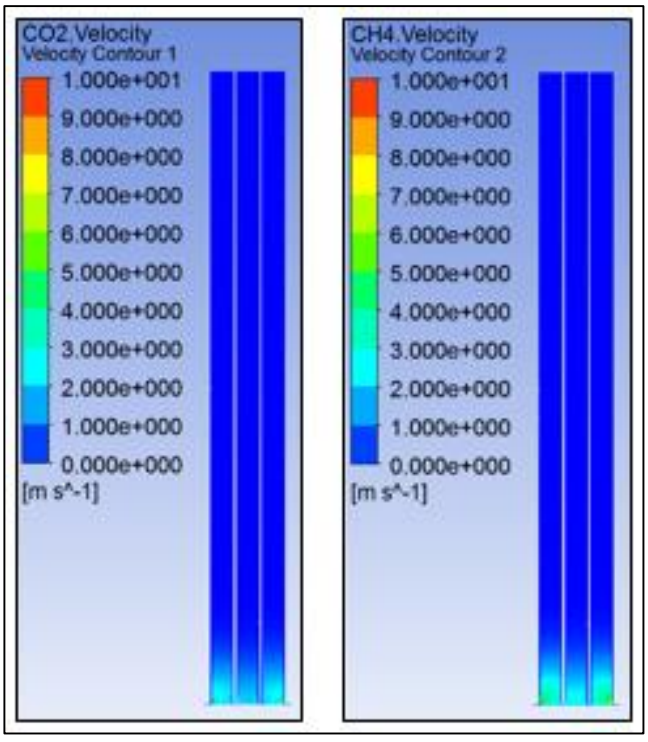

FIGURE 4.7: Geometry 2 Contour

The velocity contour is sliced at the centre of adsorption column at XY plane with coordinate of Z=0. Both fluid velocity contour showing medium velocity flowrate at the inlet of the column and reduces greatly to zero until the end of the column.

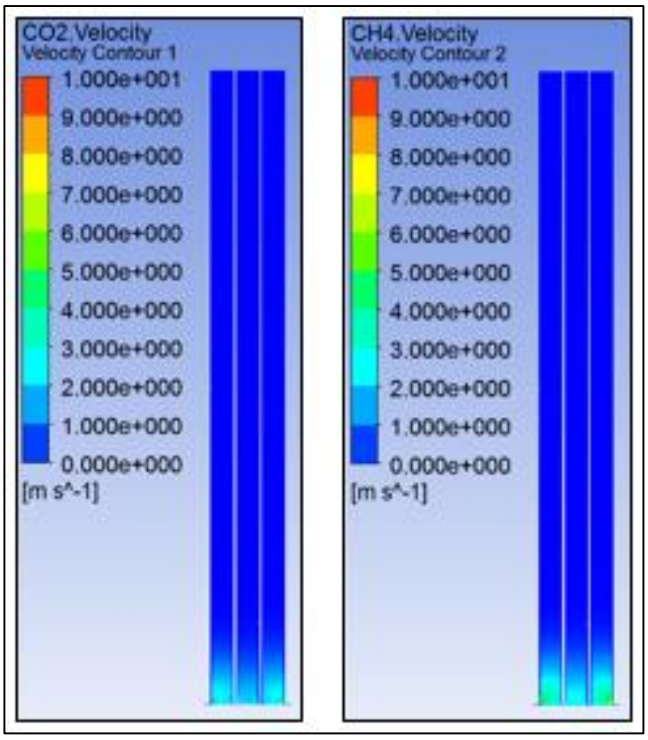

FIGURE 4.8: Geometry 3 Contour

The velocity contour is sliced at the centre of adsorption column at XY plane with coordinate of Z=0.0933 m. Both fluid velocity contour showing medium velocity flowrate at the inlet of the column and reduces greatly to zero until the end of the column.

4.1.3 Axial Velocity Graph of 250µm Particles Diameter

a) Geometry 1

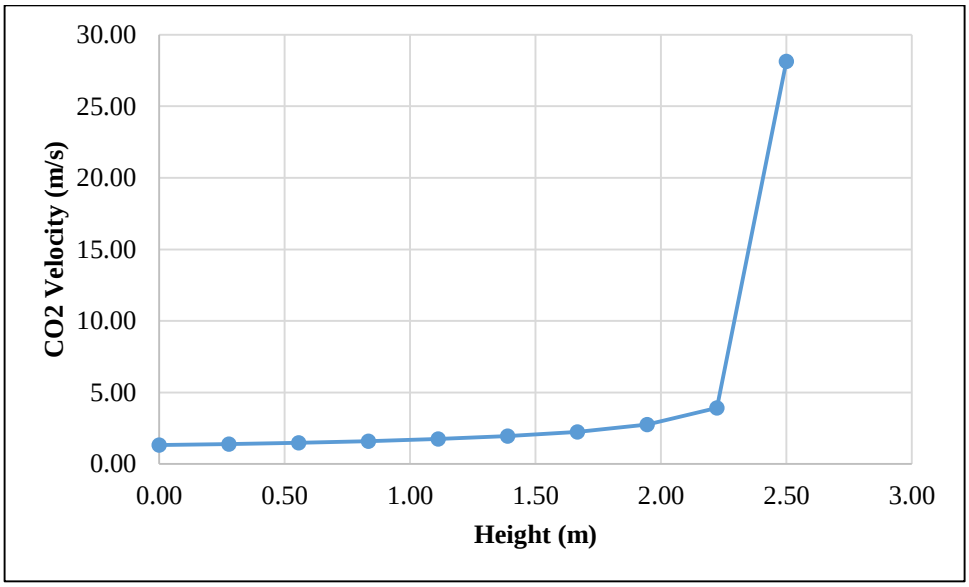

FIGURE 4.9: CO_2 velocity vs height of adsorption column for geometry 1 of 250µm

b) Geometry 2

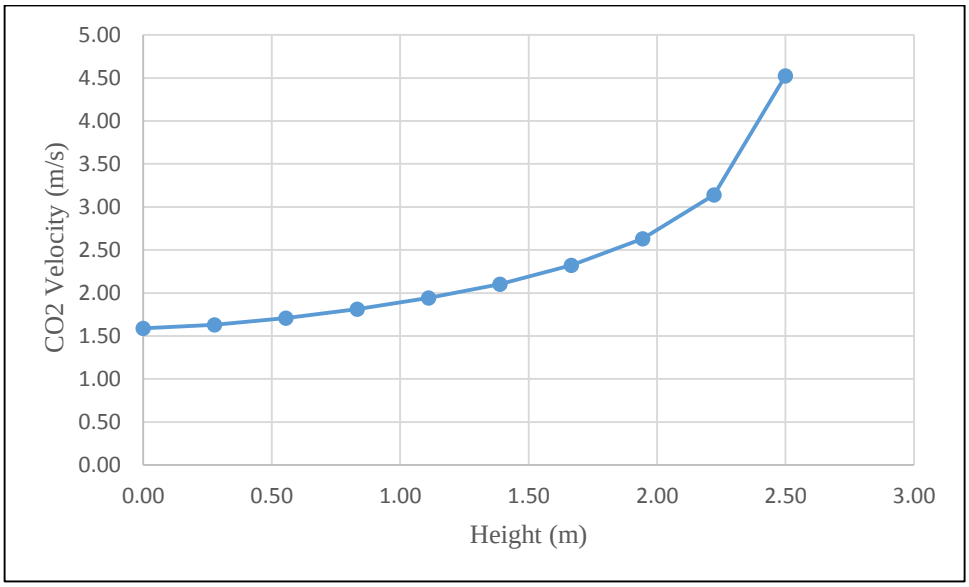

FIGURE 4.10: CO_2 velocity vs height of adsorption column for geometry 2 of 250µm

c) Geometry 3

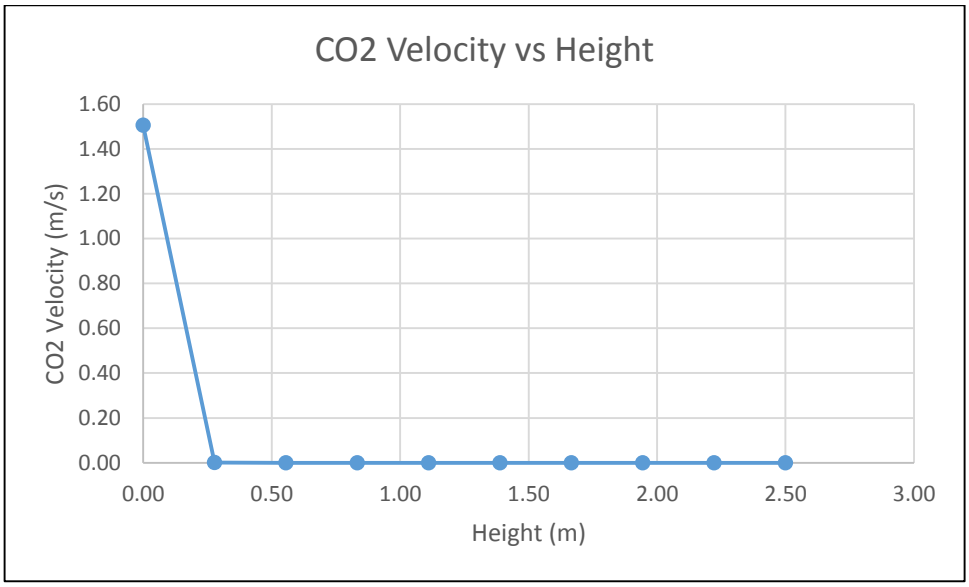

FIGURE 4.11: CO_2 velocity vs height of adsorption column for geometry 3 of 250µm

4.1.4 Axial Velocity Graph of 500µm Particles Diameter

a) Geometry 1

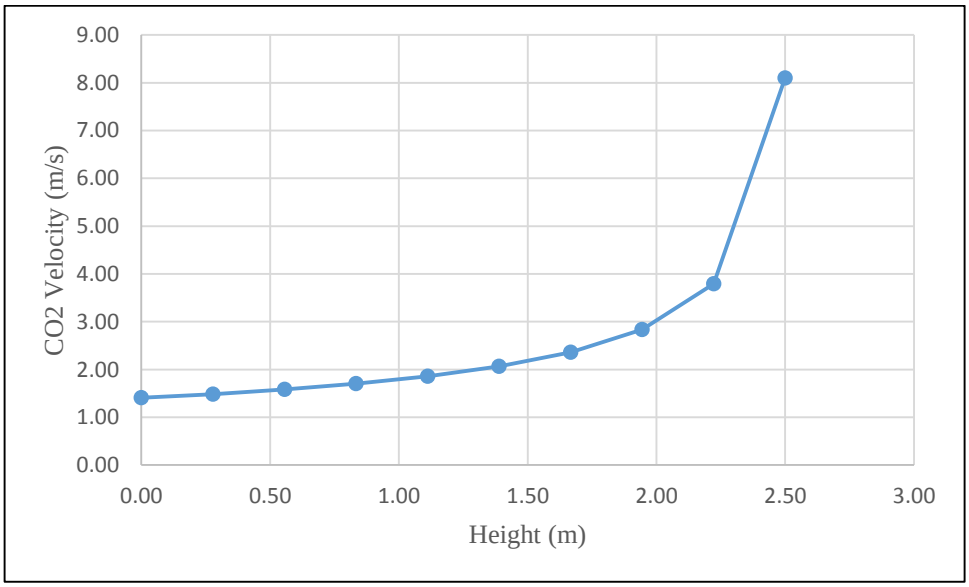

FIGURE 4.12: CO_2 velocity vs height of adsorption column for geometry 1 of 500µm

b) Geometry 2

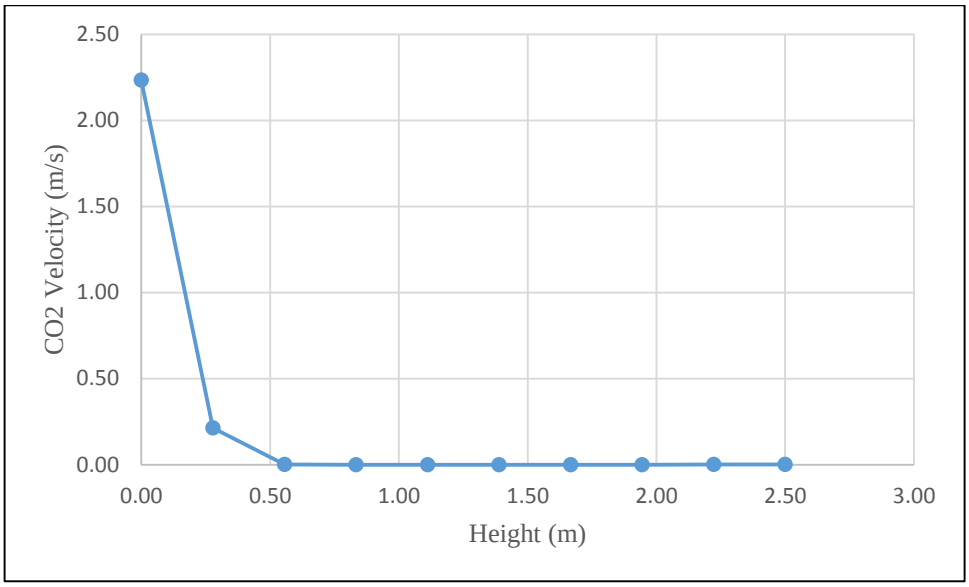

FIGURE 4.13: CO_2 velocity vs height of adsorption column for geometry 2 of 500µm

c) Geometry 3

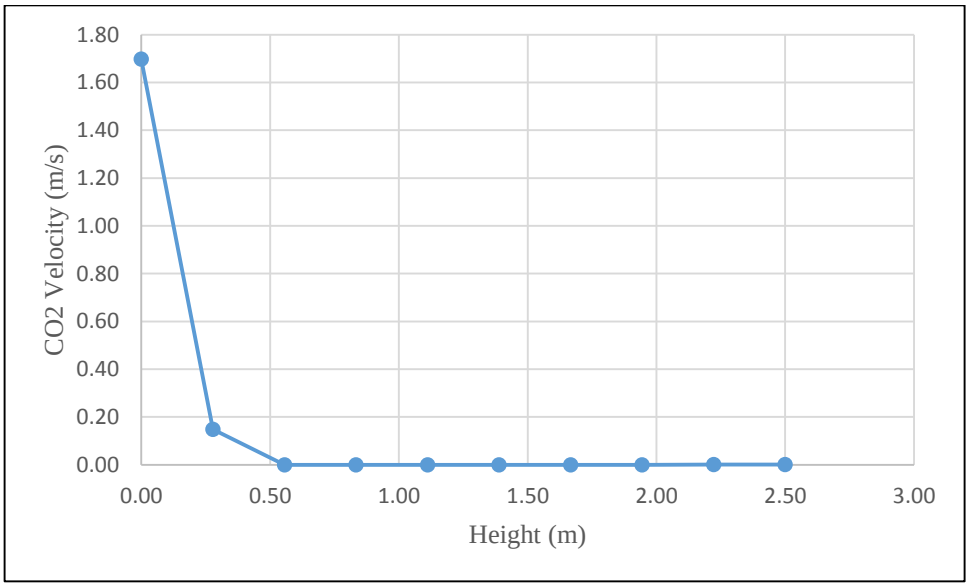

FIGURE 4.14: CO_2 velocity vs height of adsorption column for geometry 3 of 500µm

4.1.5 Radial Velocity Contour for 250µm

The radial velocity contour for CO_2 was plot at the inlet, middle and outlet to observe the velocity behavior throughout adsorption column.

a) Geometry 1

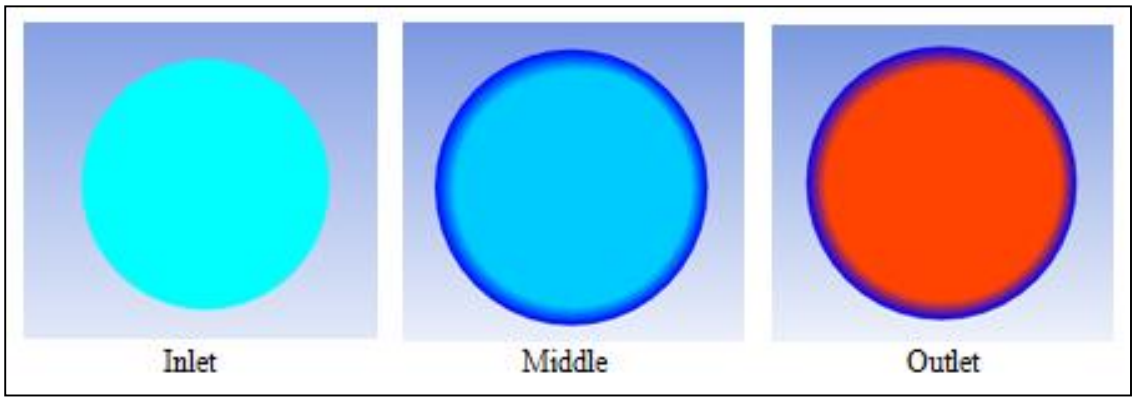

FIGURE 4.15: Radial CO_2 velocity contour plot for geometry 1

b) Geometry 2

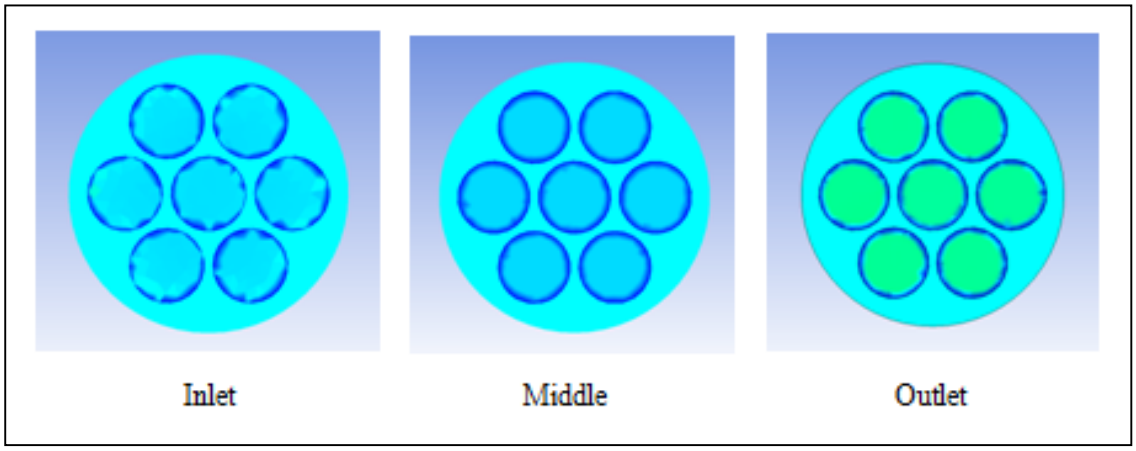

FIGURE 4.16: Radial CO_2 velocity contour plot for geometry 2

c) Geometry 3

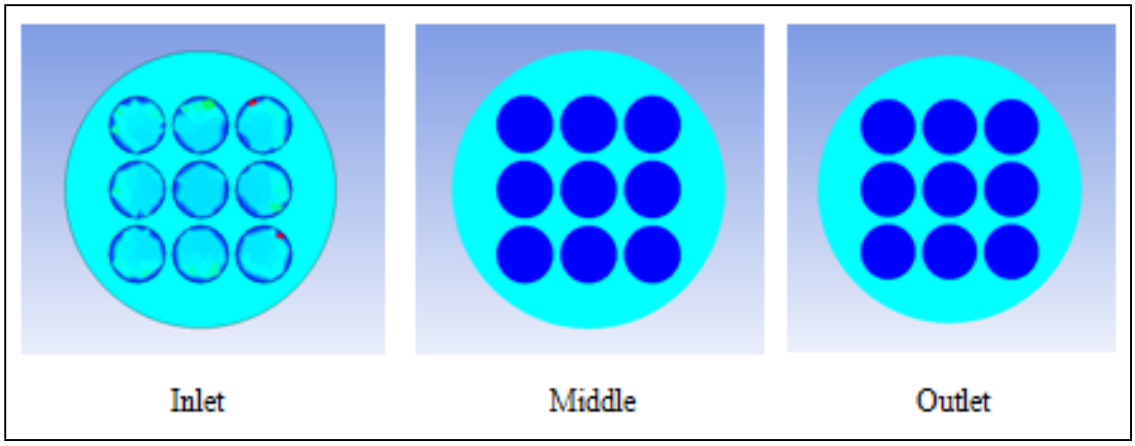

FIGURE 4.17: Radial CO_2 velocity contour plot for geometry 3

4.1.6 Radial Velocity Contour for 500µm

a) Geometry 1

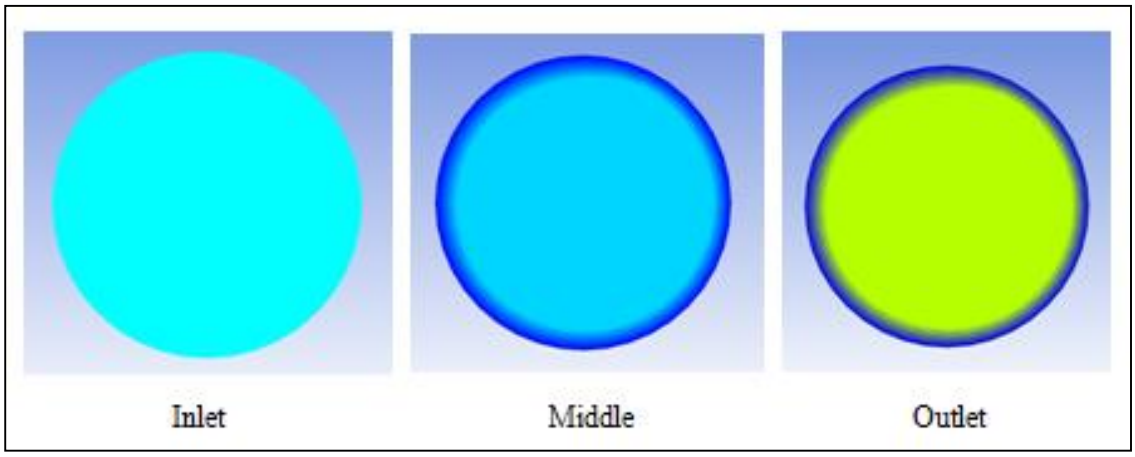

FIGURE 4.18: Radial CO_2 velocity contour plot for geometry 1

b) Geometry 2

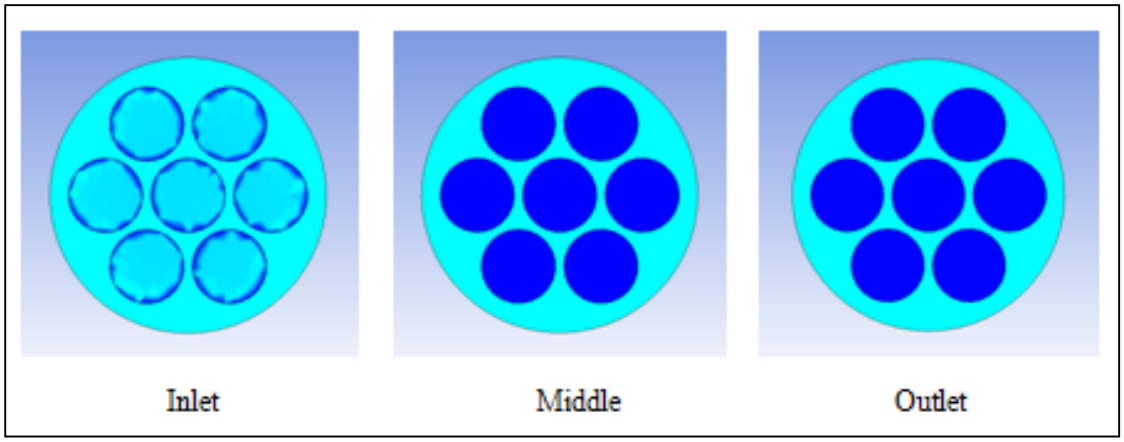

FIGURE 4.19: Radial CO_2 velocity contour plot for geometry 2

c) Geometry 3

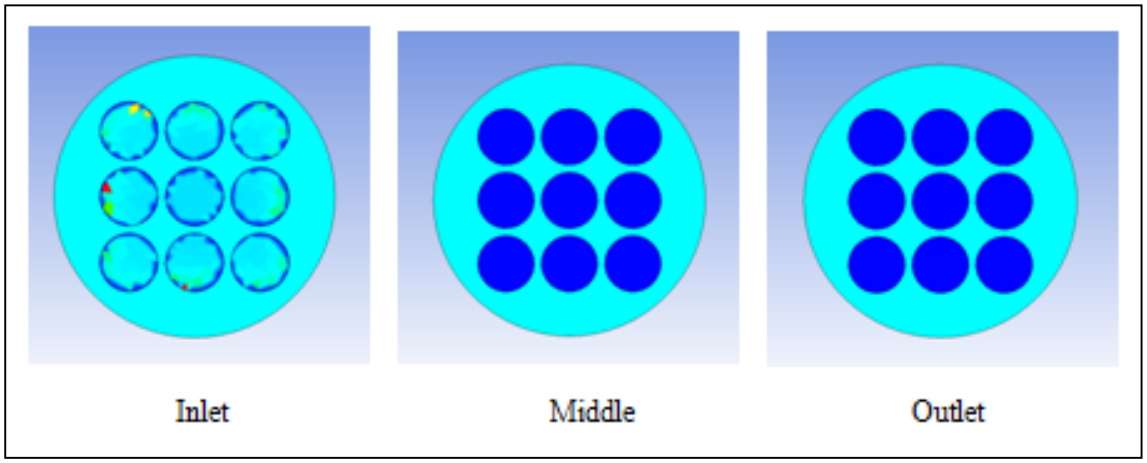

FIGURE 4.20: Radial CO_2 velocity contour plot for geometry 3

4.1.7 Radial Velocity Profile for 250µm

a) Geometry 1

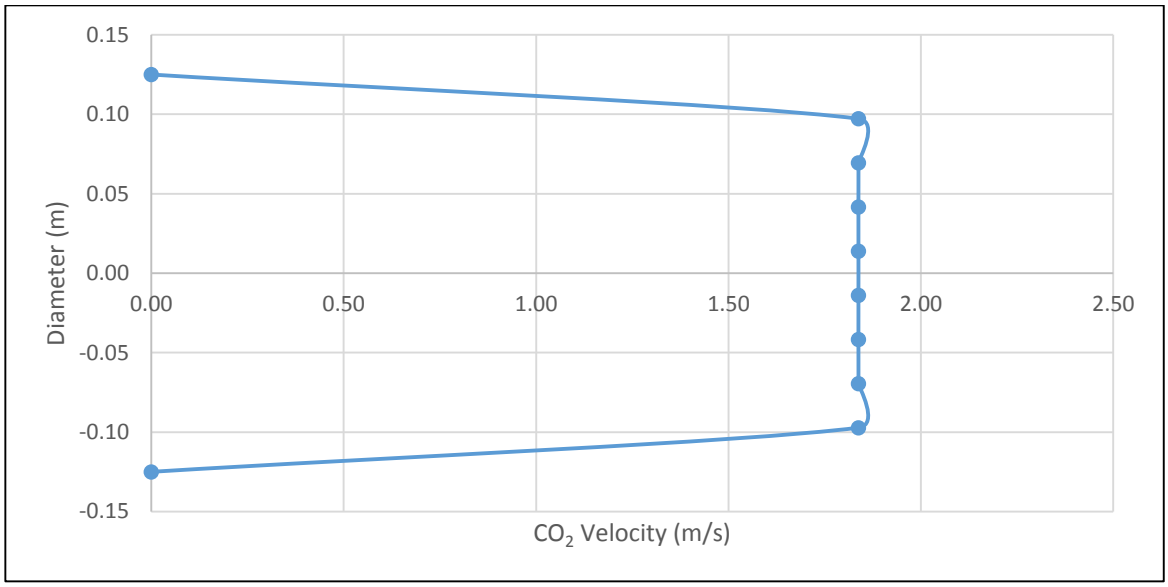

FIGURE 4.21: Radial CO_2 velocity profiles diameter of column for geometry 1 of 250µm

b) Geometry 2

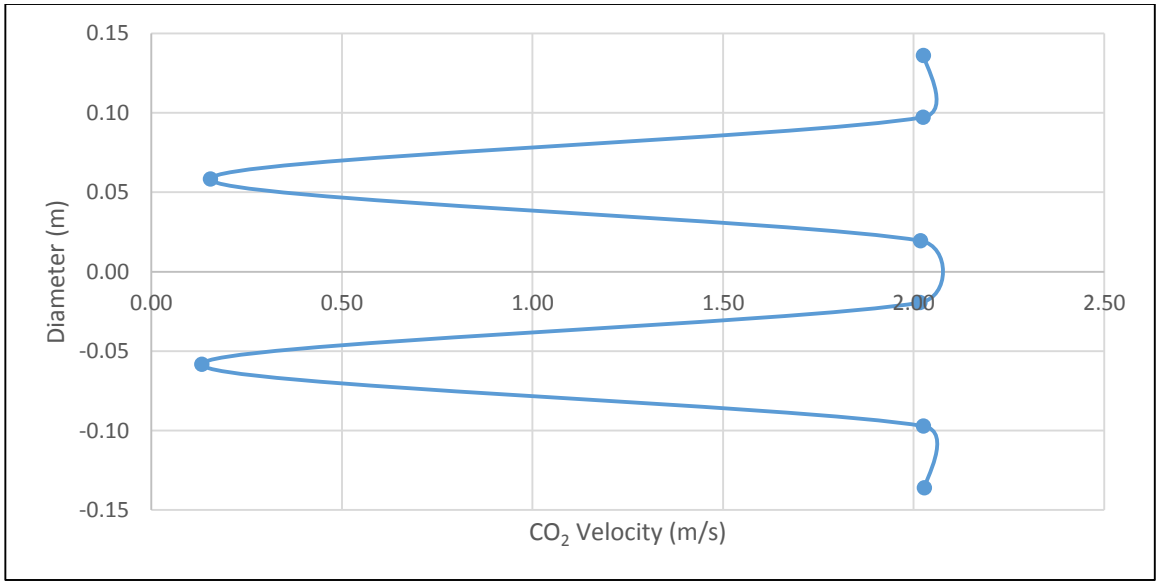

FIGURE 4.22: Radial CO_2 velocity profile vs diameter of column for geometry 2 of 250µm

c) Geometry 3

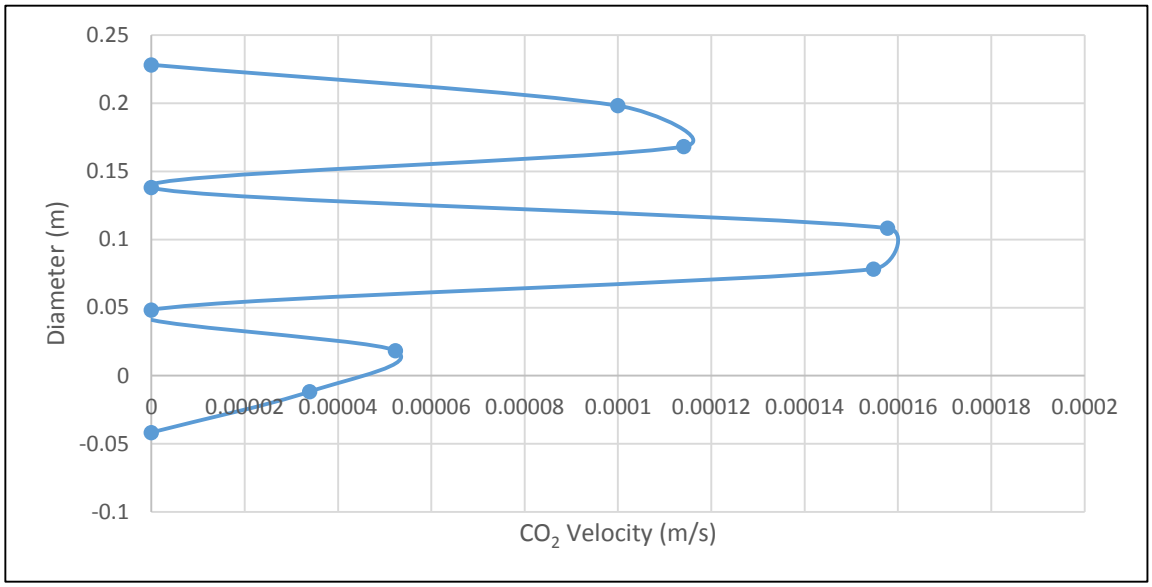

FIGURE 4.23: Radial CO_2 velocity profile vs diameter of column for geometry 3 of 250µm

4.1.8 Radial Velocity Profile for 500µm

a) Geometry 1

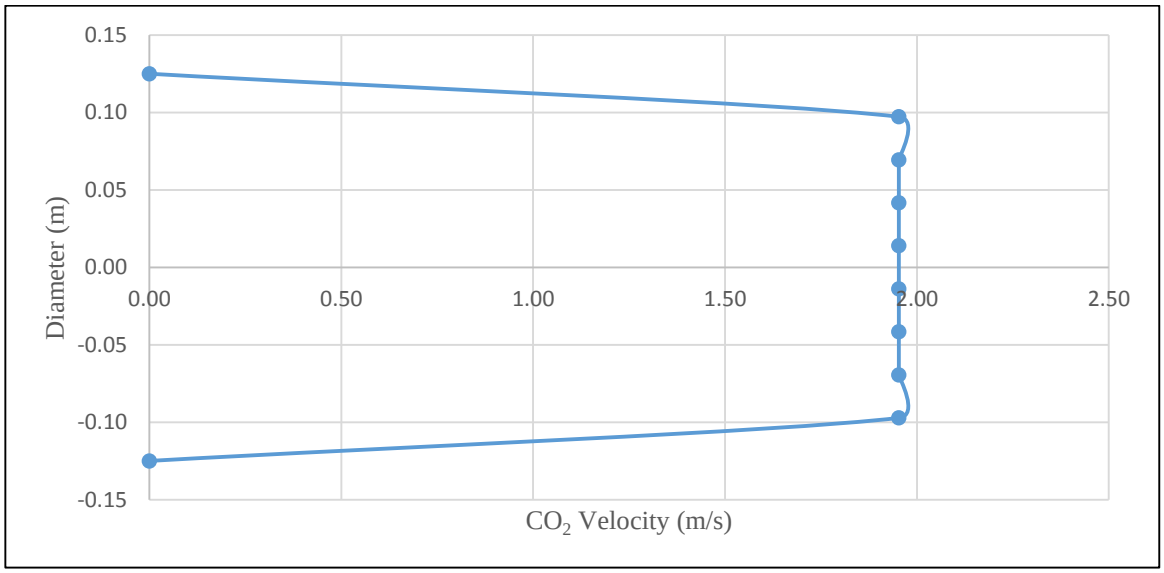

FIGURE 4.24: Radial CO_2 velocity profile vs diameter of column for geometry 1of 500µm

b) Geometry 2

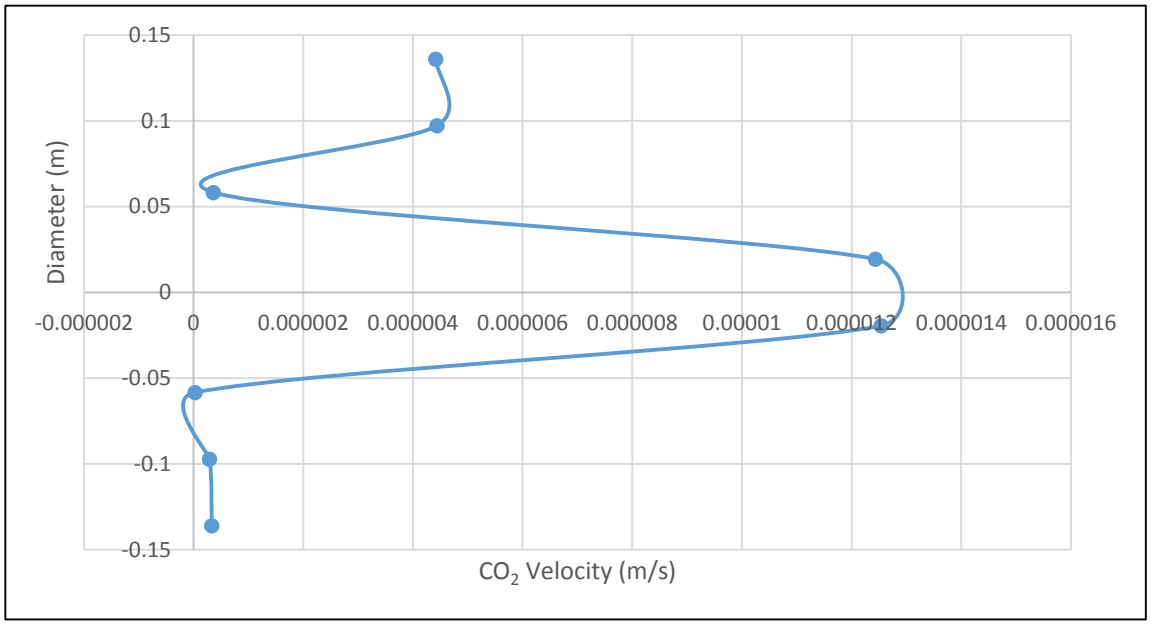

FIGURE 4.25: Radial CO_2 velocity profile vs diameter of column for geometry 2 of 500µm

c) Geometry 3

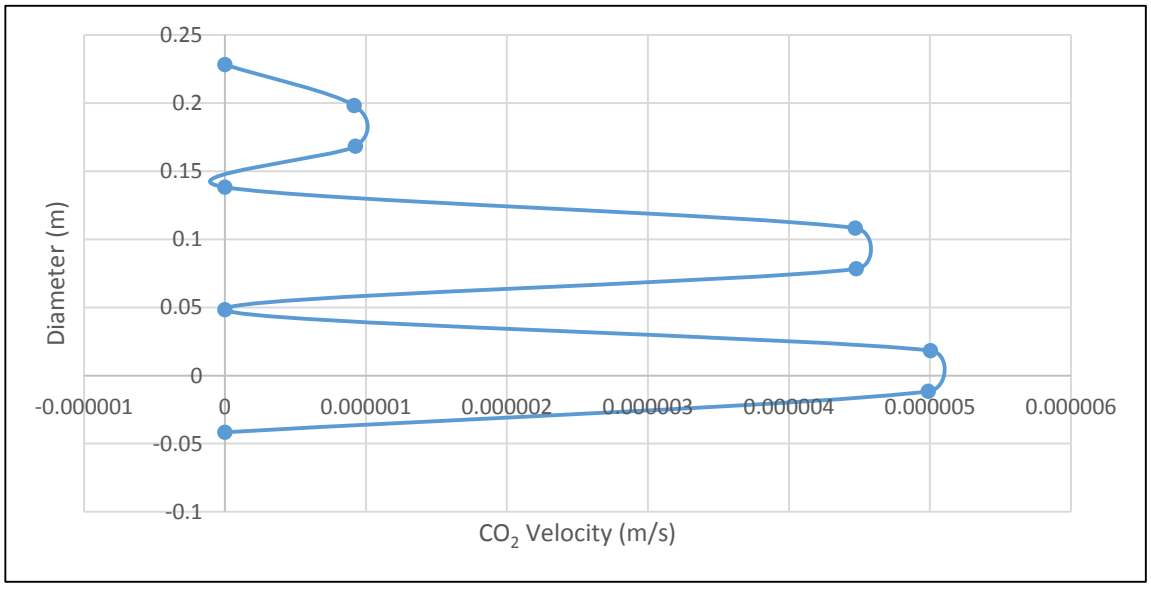

FIGURE 4.26: Radial CO_2 velocity profile vs diameter of column for geometry 3 of 500µm

4.2 Pressure Distribution in Adsorption Column

The pressure gradient defines the acceleration of gas due to the pressure difference and where the rate of pressure differ greatly around a specific location in the adsorption column. Pressure drop is a vital parameter of fluid flow to estimate the necessary energy consumption throughout adsorption column. Theoretically, pressure in the adsorption column decreases in the direction of fluid velocity along the axial direction. The pressure gradient is critically depends upon the factors of permeability and resistance coefficient along with viscosity, density and inlet velocity of the fluid. These two parameter is calculated based on Ergun's equation as discussed before.

4.2.1 Total Pressure Using 250µm Particle Diameter

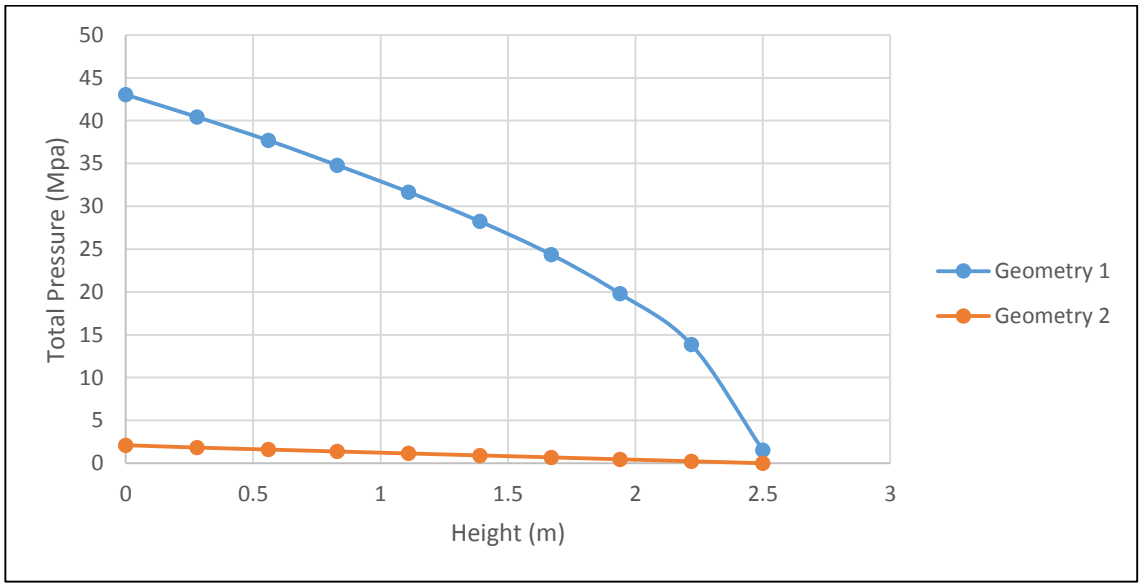

FIGURE 4.27: Total pressure vs height for geometry 1 and geometry 2

Based on Figure 4.27, the total pressure for geometry 1 and geometry 2 was tabulated meanwhile the total pressure for geometry 3 cannot be shown in the graph because the value calculated is too small.

4.2.2 Total Pressure Using 500µm Particle Diameter

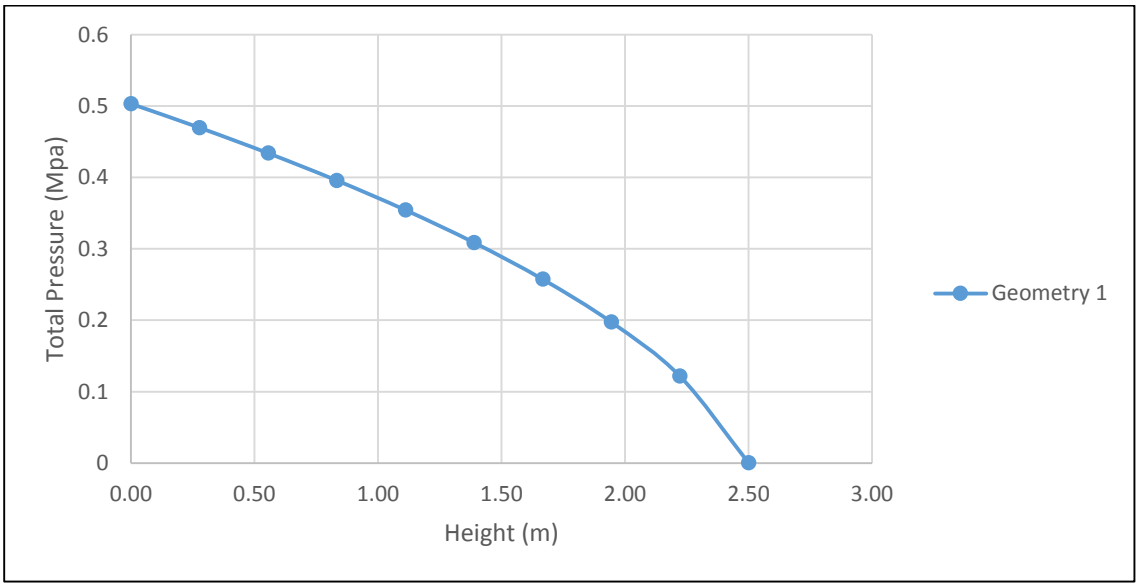

FIGURE 4.28: Total pressure vs height for geometry 1

Based on Figure 4.28, the total pressure of geometry 1 showing a huge decrease along the height of the column meanwhile total pressure for geometry 1 and geometry 2 cannot be shown because relatively too small to be shown in the graph.

4.2.3 Total Pressure between Geometries

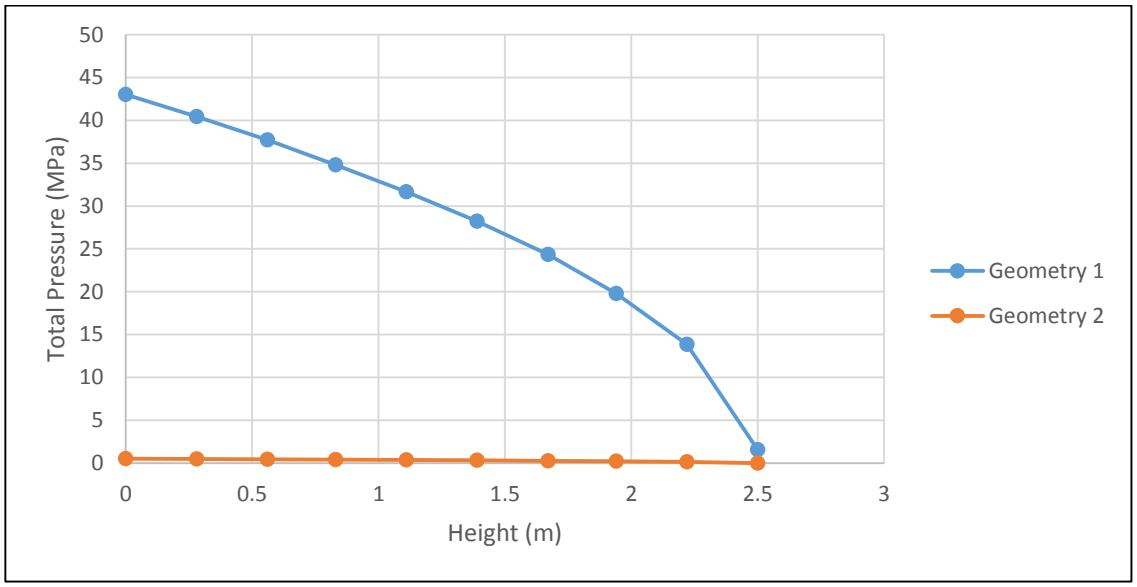

FIGURE 4.29: Total pressure vs height for geometry 1 using 250µm and 500µm

Figure 4.29 showing total pressure of geometry 1 using 250µm and 500µm respectively. The total pressure for other geometries cannot be shown because of relatively small values to be plotted in graph. There is major total pressure difference between columns that using 250µm particle diameter and 500µm particle diameter. Geometry with smaller particle diameter showing huge total pressure margin decrease compared to the geometry with larger particle diameter.

4.2.4 Axial Pressure Contour Using 250µm

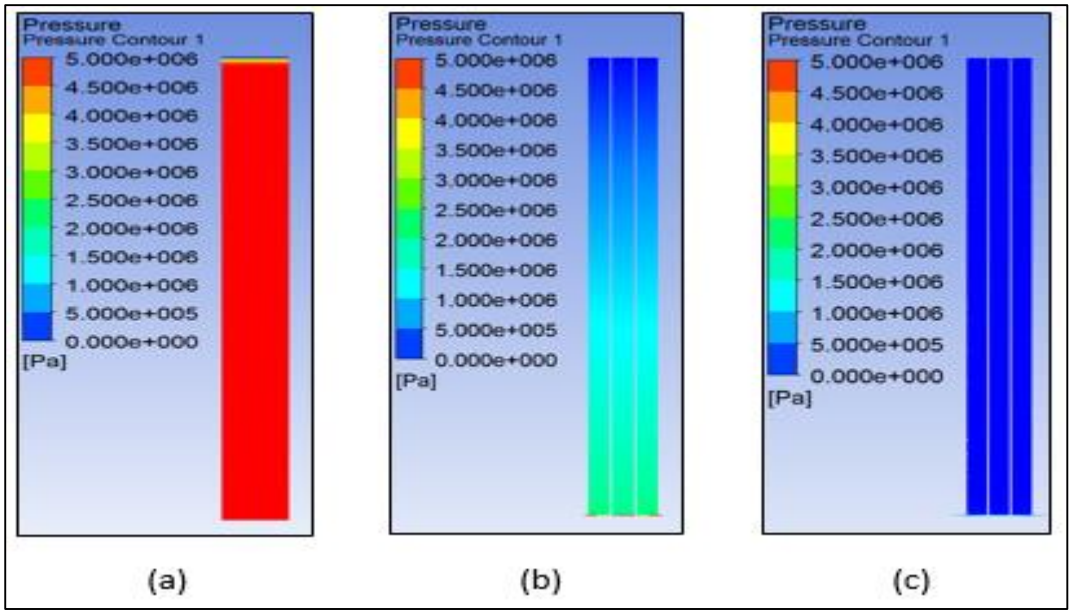

FIGURE 4.30: Axial pressure contour for different geometries for 250µm (a) Geometry 1 (b) Geometry 2 (c) Geometry 3

4.2.5 Axial Pressure Contour Using 500µm

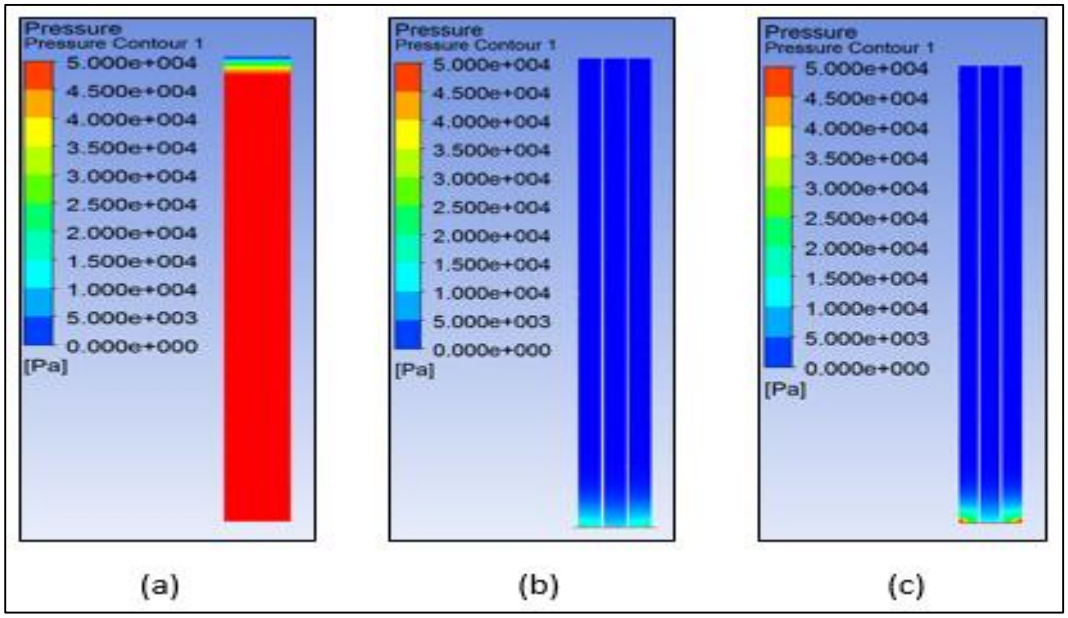

FIGURE 4.31: Axial pressure contour for different geometries for 500µm (a) Geometry 1 (b) Geometry 2 (c) Geometry 3

4.3 Discussion

Based on the simulated results of the adsorption column through ANSYS CFX software, the values obtained is a relation between the shape of geometries and also particles diameter sizes used. Adsorption column using 250μm particles diameter produces a higher values in term of velocity and pressure distribution along the column compared to the column using 500μm particles diameter. The geometry of the columns also gave indication that a solid cylinder geometry is more consistent in producing the results of velocity and pressure behavior aspect compared to the circular shape multi-cylinder and rectangular shape multi-cylinder. This is because of velocity and pressure were distributed between the small multi-cylinder along the column and yields a results that is not consistent with the one solid cylinder adsorption column. In case of rectangular multi-cylinder, the pressure and velocity were distributed in rectangular shape along the column while velocity and pressure for circular multi-cylinder is distributed in triangle shape along the column. The true velocity of the column which is also interstitial velocity is higher than the superficial velocity. This is because in porous medium, interstitial velocity is always higher than superficial velocity or known as surface velocity.

CHAPTER 5: CONCLUSION

In this study, the flow dynamics of the mixed flow CO_2/CH_4 gases through adsorption column is being investigated by implementing a numerical computational flow dynamics model through ANSYS CFX. The behavior of interstitial velocity or known as true velocity and total pressure inside adsorption column is being examined by observing the changes in column contour and graph distribution along the column height. The axial and radial velocity is examined for 250μm and 500μm between 3 geometry models. Based on the graphs, small particle diameter is showing higher value of velocity compared to bigger particle diameter but the differences is minimal. The highest total pressure is shown by 250μm particle diameter and become lesser when 500μm particle diameter is used. The geometry dimensions and shapes give more significant changes in term of velocity and pressure change compared to the increasing of particles diameter size.

REFERENCES

[1] S.A Nouh, K.K. Lau and A.M. Shariff. "Modelling and simulation of fixed bed adsorption column using integrated CFD approach",*Journal of Applied Sciences,*10(24), 3229-3235, 2010.

[2] M.G. Plaza, C. Pevida, B. Arias, J. Fermoso, M.D. Casal, C.F. Martin et al. "Development of low-cost biomass-based adsorbents for postcombustion CO_2 capture",*Fuel*, 88(12), 2442-2447, 2009.

[3] M.G. Plaza, S. Garcia, F. Rubiera, J.J. Pis, C. Pevida. "Evaluation of ammonia modified and conventionally activated biomass based carbons as CO_2adsorbents in postcombustion conditions",*Separation and Purification Technology*, 80(1): 96-104, 2011.

[4] A. Olajire. "CO_2 capture and separation technologies for end-of-pipe applications -A review", *Energy*, 35(6), 2610-2628, 2010.

[5] M.T. Ho, G.W. Allinson, D.E. Wiley. "Reducing the cost of CO_2 capture from flue gases using pressure swing adsorption", *Ind. Eng. Chem. Res.*47: 4883-4890, Malaysian Palm Oil Board,2009.

[6] R. Serna-Guerrero and A. Sayari. "Modelling adsorption of CO_2 on amine functionalizedmesoporous silica. 2: Kinetics and breakthrough curves", *Chemical Engineering Journal*, 161: 182-190, 2010.

[7] H. P. S. Abdul Khalil, M. J., P. Firoozian, Umer Rashid, Aminul Islam, and Hazizan Md. Akil. "Activated Carbon from Various Agricultural Wastes by Chemical Activation with KOH: Preparation and Characterization"*Journal of Biobased Materials and Bioenergy*, Vol. 7, 1-7, 2013.

[8] Sunho Choi, J. H. D., and Christopher W. Jones. “Adsorbent Materials for Carbon Dioxide Capture from Large Anthropogenic Point Sources”, *ChemSusChem.*, Vol. 2, 796-854, 2009.

[9] Hongqun Yang, Z. X., Maohong Fan2, Rajender Gupta, Rachid B Slimane, Alan E Bland, Ian Wright. “Progress in carbon dioxide separation and capture: A review”, *Journal of Environmental Sciences*, 20, 14-27, 2008.

[10] Jamaludin, S. R. B., "A Production Of Activated Carbon Using Local Agricultural Waste For Groundwater Treatment″Ph. D. dissertation, Universiti Malaysia Pahang, Bachelor of Civil Engineering Department, 2012.

[11] M. Zamri Abdullah, S. A. Q. Z. “Computational Modelling And Optimization Of Utilization Of Nanoporous Adsorbent From Agricultural Waste For Carbon Dioxide Capture”, Universiti Teknologi Petronas, Bachelor of Chemical Engineering Department, 2014.

[12] Mohsen Hamidipour, J., Faical Larachi. "CFD study on hydrodynamics in three-phase fluidized beds—Application of turbulence models and experimental validation". *Chemical Engineering Science 78*, 167-180, 2012.

[13] W. Kangwanwatana, C. Saiwan, and P. Tontiwachwuthikul. “Study of CO_2 AdsorptionUsing Adsorbent Modified with Piperazine*”*, *Chemical Engineering Transactions*, Vol. 35, 403 – 408,2013.

[14] M.M. Maroto-Valer, Z. Tang, and Y. Zhang. “CO_2 Capture By Activated And Impregnated Anthracites”, *Fuel Processing Technology*, 86, 1487-1502, 2005.

APPENDICES

Appendix A-1

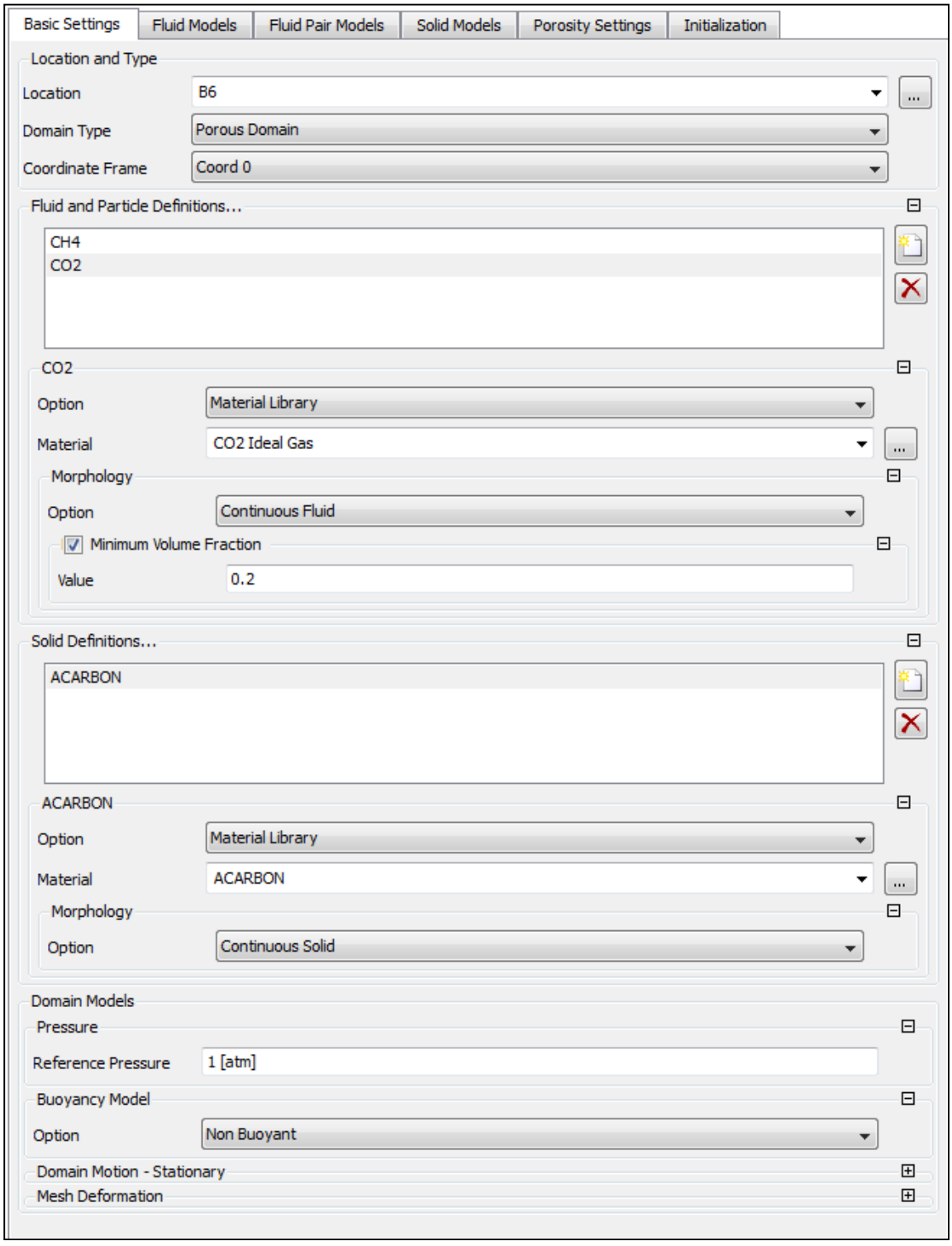

Appendix A-2

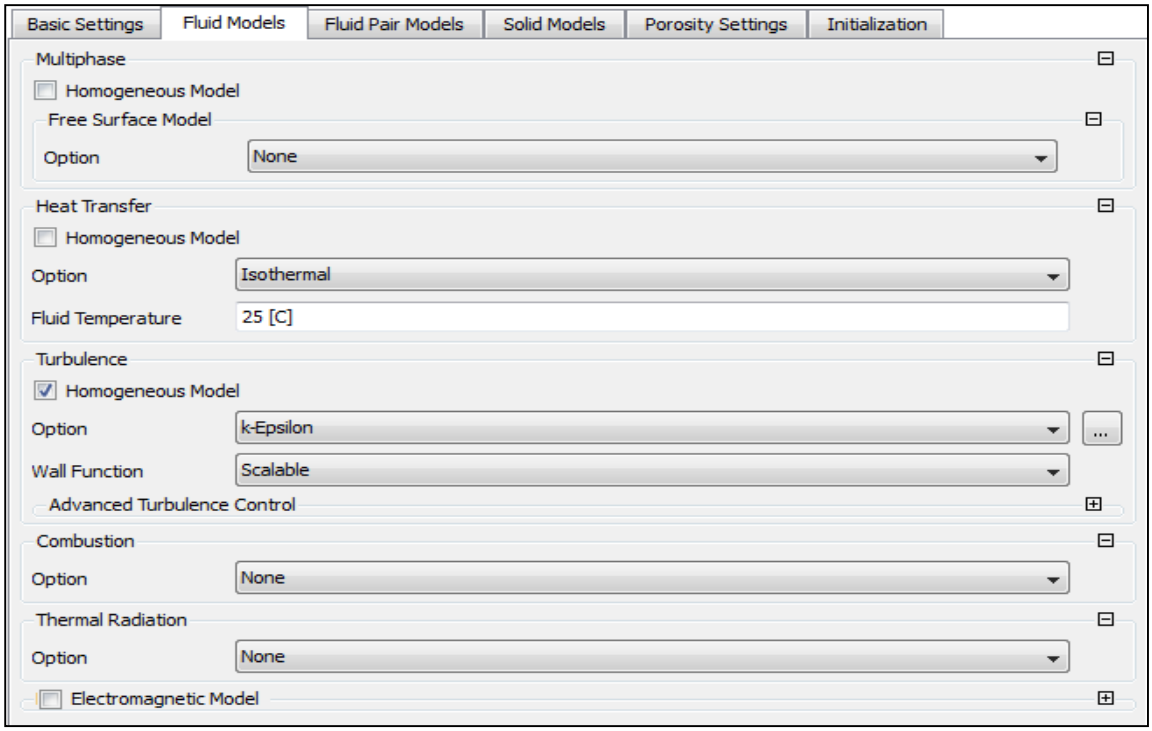

Appendix A-3

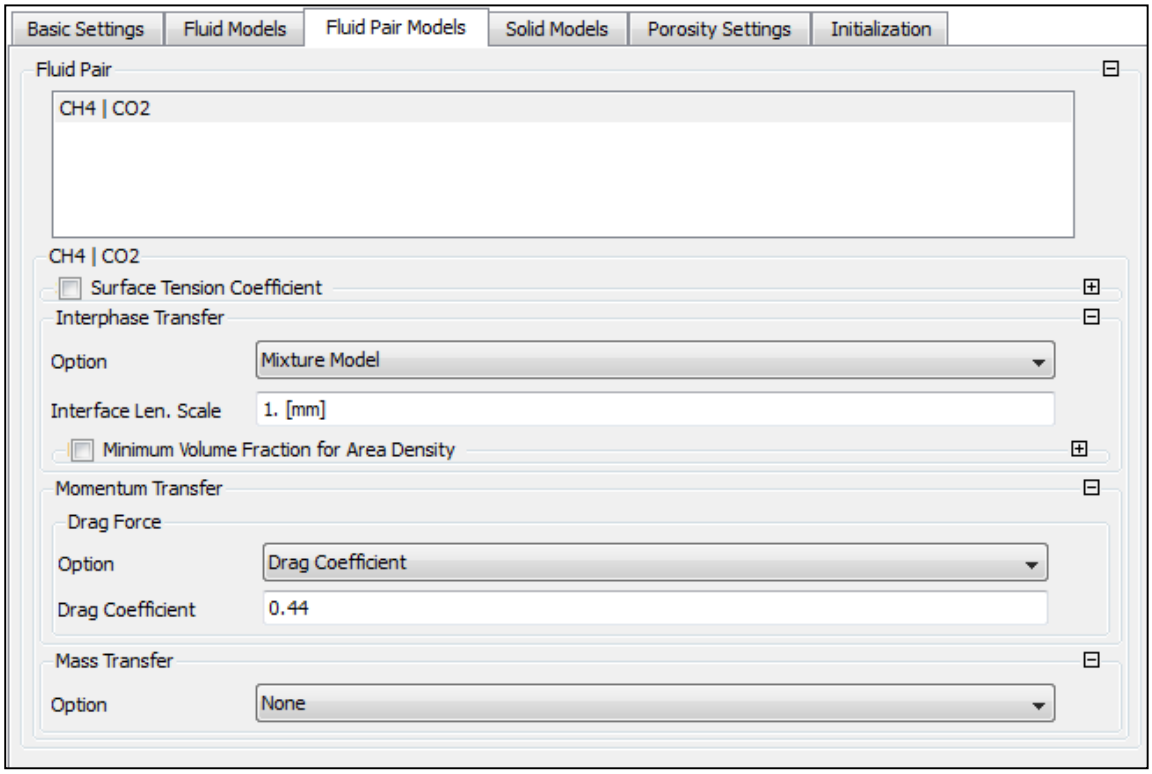

Appendix A-4

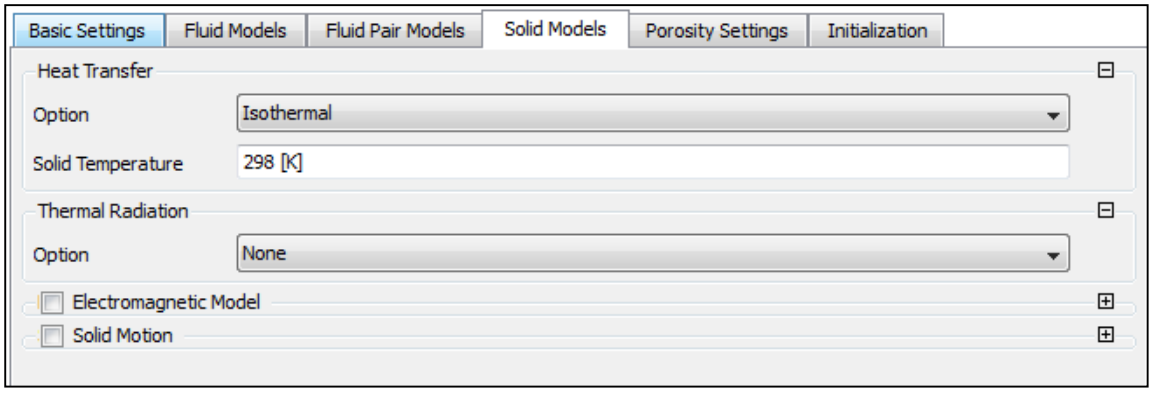

Appendix A-5

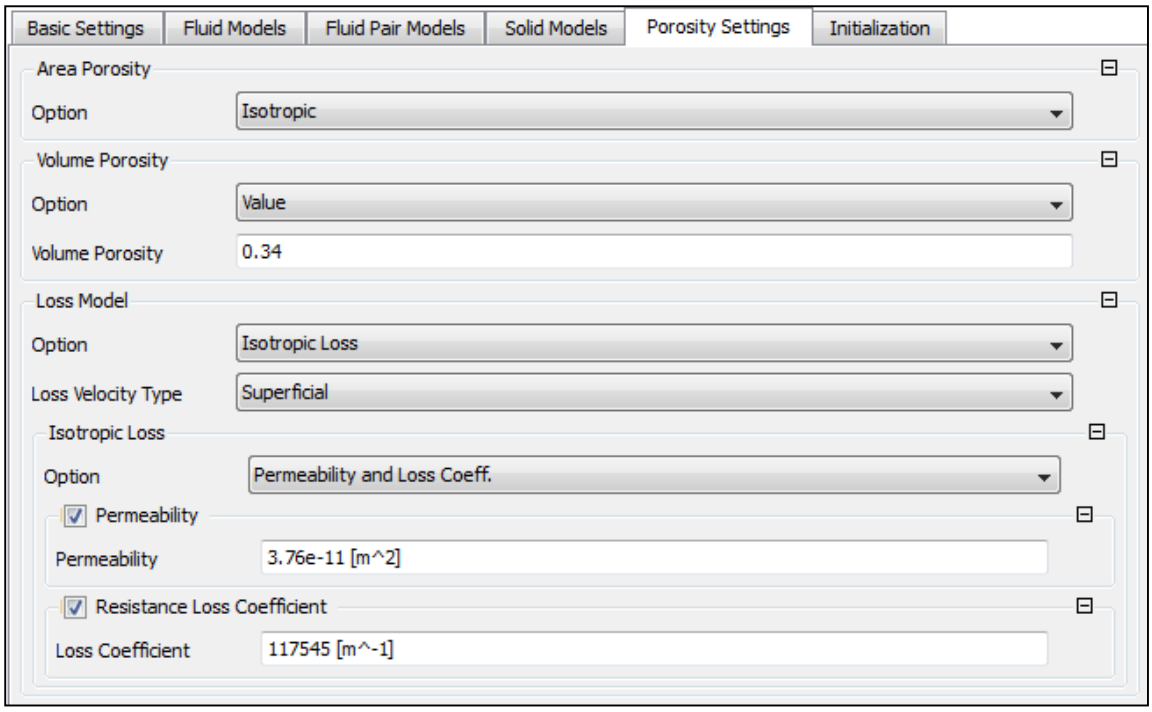

Appendix A-6

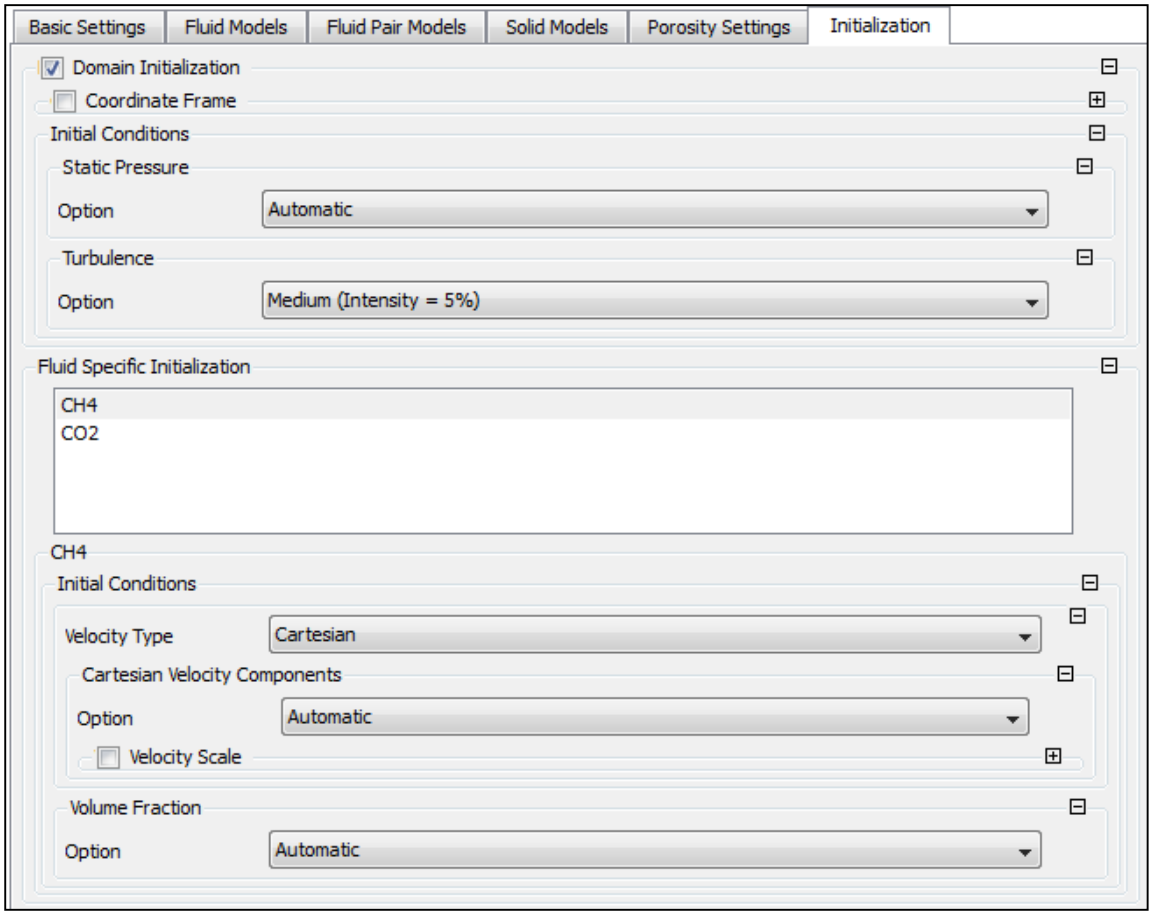
Basic Settings
Fluid Models
Fluid Pair Models
Solid Models
Porosity Settings
Initialization
Domain Initialization
Coordinate Frame
Initial Conditions
Static Pressure
Option
Automatic
Turbulence
Option
Medium (Intensity = 5%)
Fluid Specific Initialization
CH4
CO2
CH4
Initial Conditions
Velocity Type
Cartesian
Cartesian Velocity Components
Option
Automatic
Velocity Scale
Volume Fraction
Option
Automatic

Appendix B-1

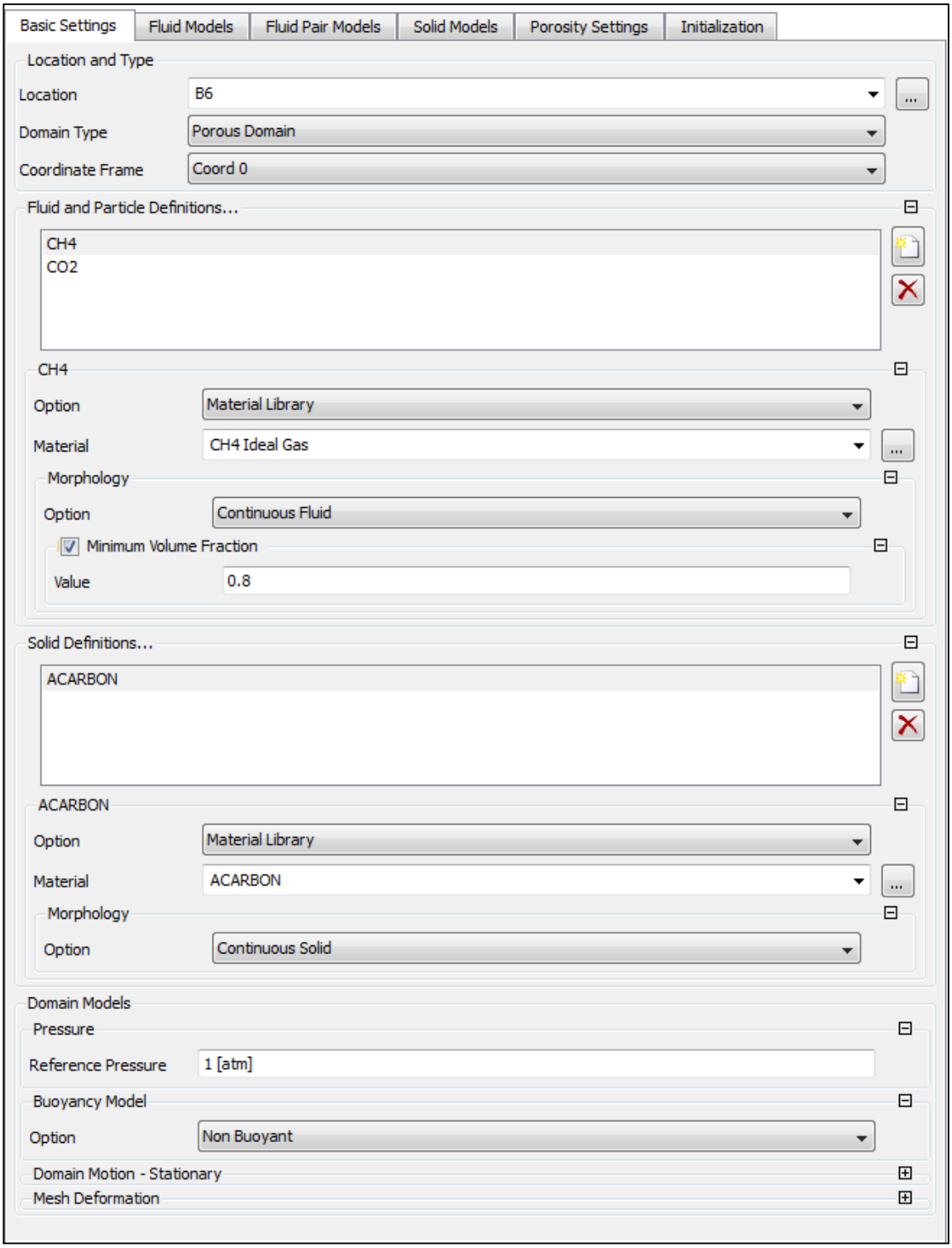
Basic Settings
Fluid Models
Fluid Pair Models
Solid Models
Porosity Settings
Initialization
Location and Type
Location
B6
Domain Type
Porous Domain
Coordinate Frame
Coord 0
Fluid and Particle Definitions...
CH4
CO2
CH4
Option
Material Library
Material
CH4 Ideal Gas
Morphology
Option
Continuous Fluid
Minimum Volume Fraction
Value
0.8
Solid Definitions...
ACARBON
ACARBON
Option
Material Library
Material
ACARBON
Morphology
Option
Continuous Solid
Domain Models
Pressure
Reference Pressure
1 [atm]
Buoyancy Model
Option
Non Buoyant
Domain Motion - Stationary
Mesh Deformation

Appendix B-2

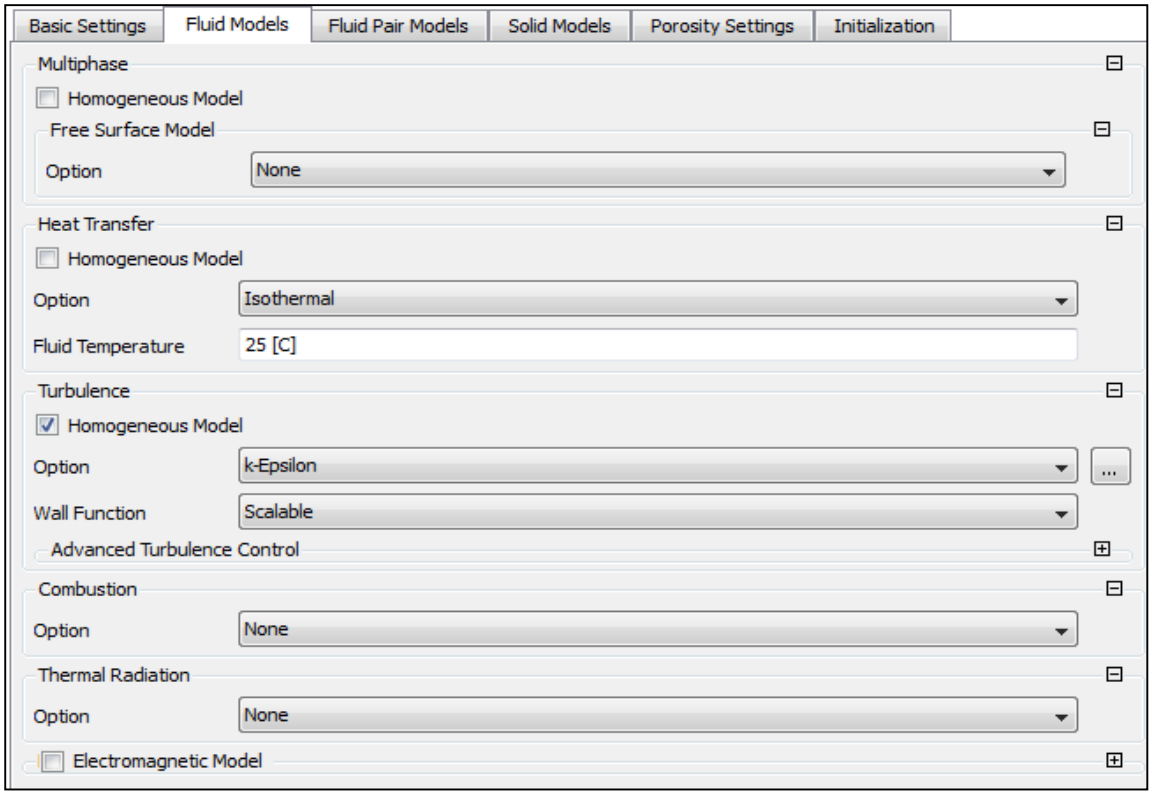

Appendix B-3

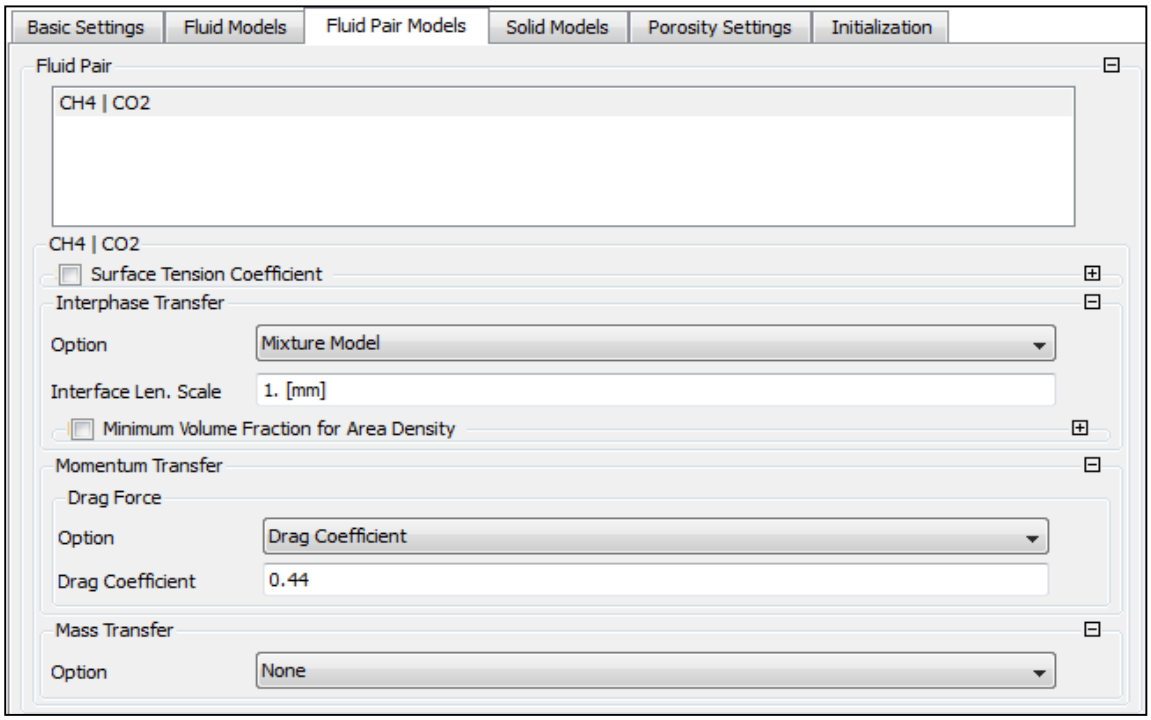

Appendix B-4

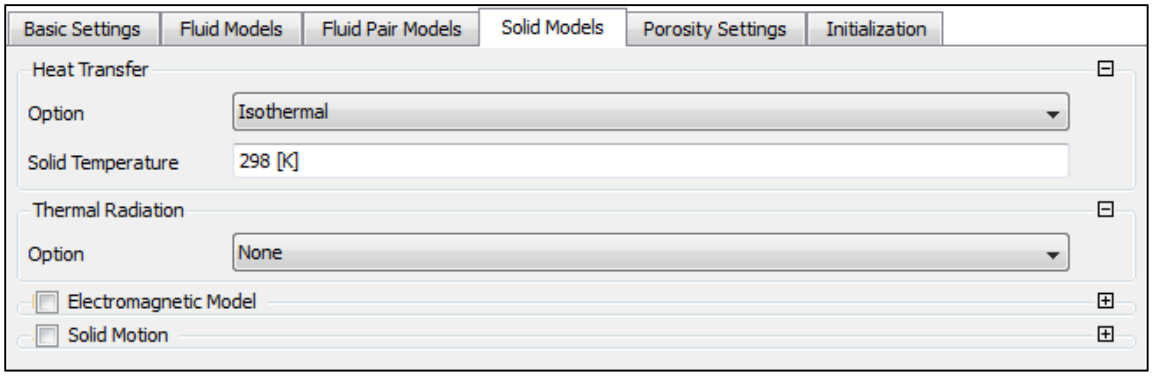

Appendix B-5

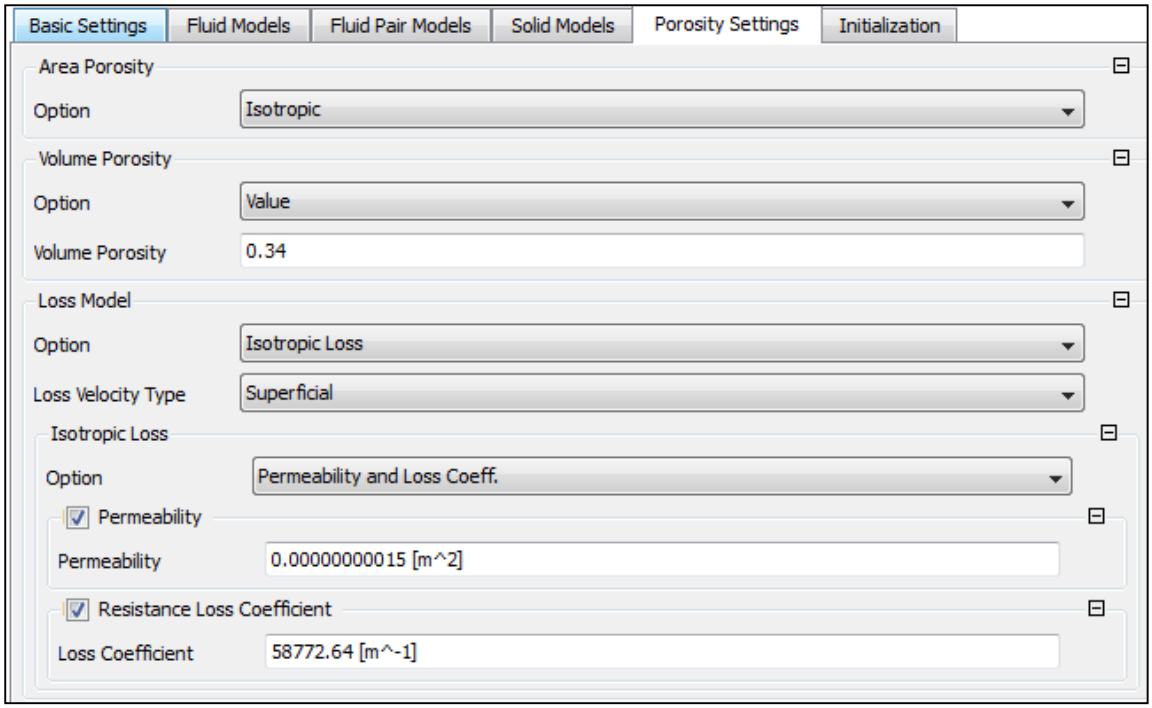

Appendix B-6

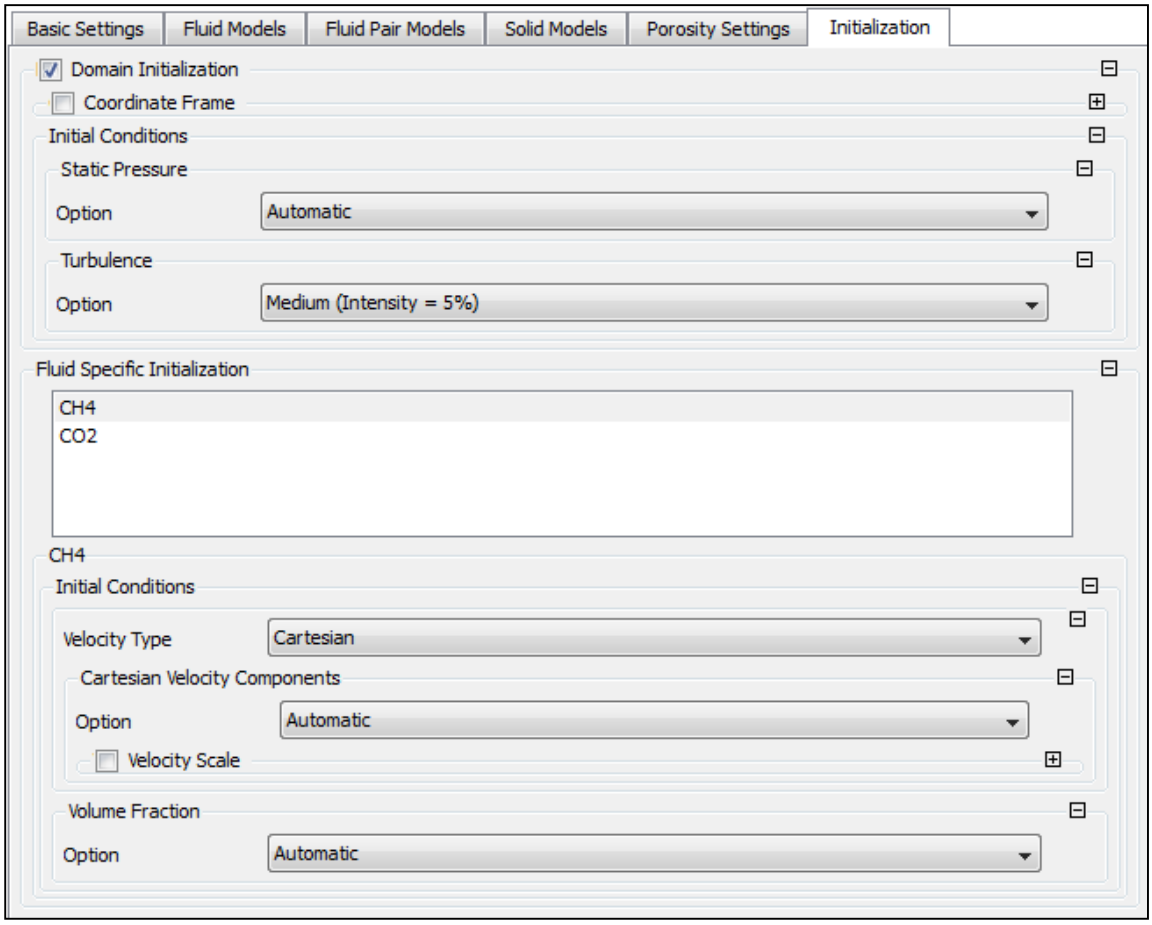
Basic Settings
Fluid Models
Fluid Pair Models
Solid Models
Porosity Settings
Initialization
Domain Initialization
Coordinate Frame
Initial Conditions
Static Pressure
Option
Automatic
Turbulence
Option
Medium (Intensity = 5%)
Fluid Specific Initialization
CH4
CO2
CH4
Initial Conditions
Velocity Type
Cartesian
Cartesian Velocity Components
Option
Automatic
Velocity Scale
Volume Fraction
Option
Automatic